Since another Nkd protein in the mouse, Nkd1, can antagonize Wnt signaling in both cultured cells and in *Drosophila* embryos (Wharton et al., 2001), we determined whether *nkd1* is also expressed in the PSM and found that it exhibited an interesting expression pattern.

2.3. Mouse nkd1 mRNA oscillates in the PSM

nkd1 mRNA is first detected in the PSM and in the central nervous system of the 8.0 dpc embryo (Fig. 3A,B). In the 10.5 dpc embryo, *nkd1* expression is then observed in newly formed somites and in the neural tube, and was found to be maintained in the PSM (Fig. 3C). However, this expression pattern in the PSM varied among embryos and the signal was detected in either the middle of the PSM and tailbud (Fig. 3D) or in the more anterior PSM without tailbud (Fig. 3E). This suggests that the *nkd1* expression pattern changes in a short time in the PSM. To further analyze the precise transcriptional regulation of *nkd1*, we designed an RNA probe that was complementary to intronic sequences within the *nkd1* gene. Because this probe does not hybridize to mature spliced mRNA, we could therefore exclusively detect premature *nkd1* mRNA. Using the intronic RNA probe, we detected various expression patterns of *nkd1* in 11.5 dpc embryos (Fig. 3F–H), which could be categorized into three different phases, similar to other cyclic genes (Palmeirim et al., 1997; Bessho et al., 2001; Aulehla et al., 2003): Phase I: lower *nkd1* signal intensities in the tailbud. Phase II: *nkd1* transcripts are evident in the middle of the PSM in addition to the tailbud. Phase III: the *nkd1* signals shift more anteriorly. These results indicate that *nkd1* expression oscillates in the PSM during somitogenesis. However, another member of this family of genes, *nkd2* did not exhibit such periodic expression, although its expression was observed in the PSM (Fig. 2).

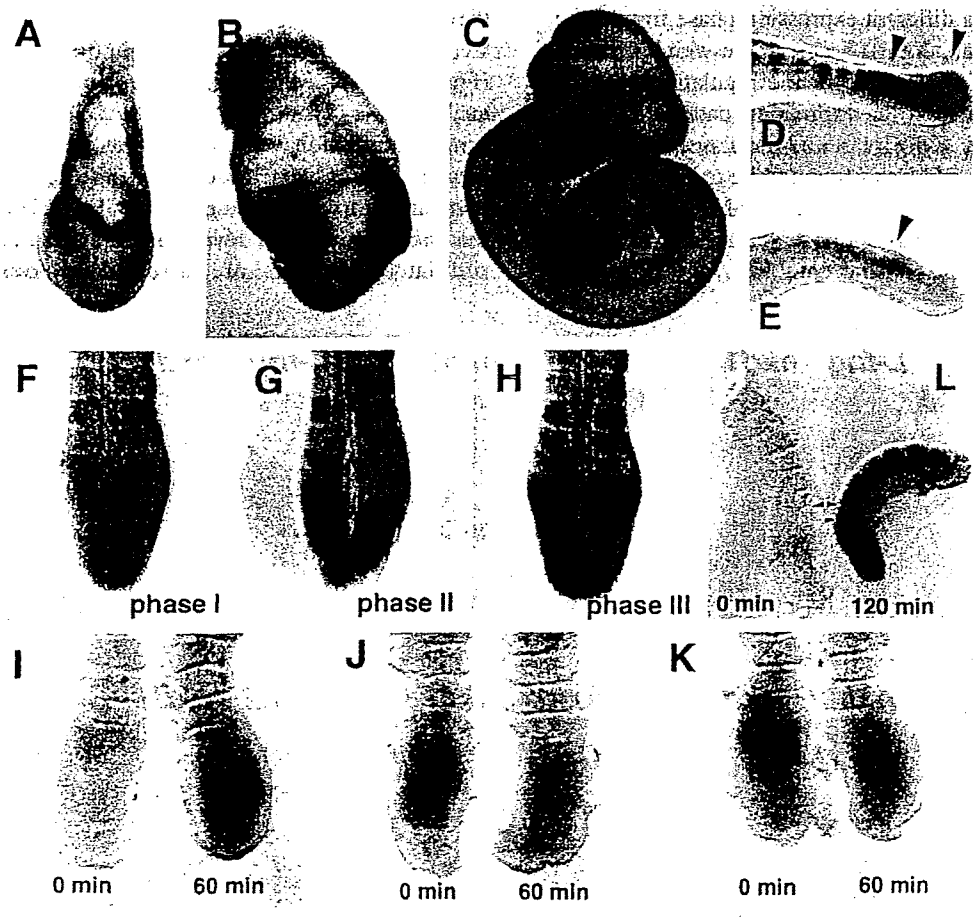

Fig. 3. Expression patterns of mouse *nkd1*. *nkd1* mRNA was detected with an exon probe at 7.5 dpc (A), 8.5 dpc (B), 10.5 dpc (C–E). *nkd1* transcripts are first detected in the central nervous system and in the PSM of 8.5 dpc embryos (B). In the 10.5 dpc embryo, *nkd1* expression is detected in the neural tube, dermomyotomes, somites and the PSM (C). Different expression patterns were detected using the exon probe (D,E). Arrowheads indicate signals in the PSM. (F–H) *nkd1* transcripts were detected using an intron probe in the tail region of 11.5 dpc embryos. Note that the expression is very weak in phase I (F), becomes stronger in the middle PSM in phase II (G) and is confined to the anterior PSM in phase III (H). (I–M) An embryo half culture experiment indicating the oscillation of *nkd1* expression. The 11.5 dpc embryo tails were cut into two halves at the midline. The left side was fixed immediately and the right side was fixed after 60 min (I–K) or 120 min (L) cultivation. Black and red arrowheads in (L) indicate segment border existed at 0 min and a newly formed border after 120 min, respectively. An intron probe was used for the ISH.

To further confirm the cyclic expression profile of *nkd1*, we performed in vitro cultures of bisected PSM, by fixing one half of the isolated tissue immediately and the additional half after a period of culturing. After 60 min, the expression patterns of *nkd1* in cultured PSM cells were altered from those of the uncultured portion (Fig. 3I–K). The change was most evident in the middle to anterior PSM, where the expression was seen to go from zero to strong levels and vice versa. After 120 min, the same pattern was observed which accompanied the formation of a new somite (Fig. 3L). These observations demonstrate that *nkd1* expression oscillates in the PSM during somitogenesis.

2.4. Comparisons of nkd1 expression patterns with other oscillatory genes

There are several genes that show periodic expression patterns during somitogenesis. The Notch-signaling related genes, *L-fng* and *hes7*, are transcribed with a similar oscillatory phase (Bessho et al., 2001), whereas the Wnt inhibitor *Axin2* has a different expression phase from these factors (Aulehla et al., 2003). To elucidate which of these signaling pathways is involved in the regulation of *nkd1* expression, we compared the expression patterns of *nkd1* with those of either *L-fng* or *Axin2* in dissected embryo halves. Surprisingly, *nkd1* was found to be expressed in the same phase as *L-fng* in the middle PSM (Fig. 4A–C), although its expression was not observed as a narrow band in the anterior PSM, as is the case for *L-fng* (Fig. 4B). These expression patterns are similar to those of the *hes7* transcripts detected with an intronic probe (Bessho et al., 2003). The oscillatory expression of both *L-fng* and of *hes7* itself is negatively controlled by Hes7 (Bessho et al., 2003). Thus, it appeared possible that *nkd1* expression would also be controlled by Hes7. On the other hand, the expression domains of *nkd1* and *Axin2* were obviously out of phase (Fig. 4D–F). For example, *Axin2* expression is not highly upregulated in the middle PSM where *nkd1* is strongly detected as phase II (Fig. 4E). *nkd1* expression is also detected as phase III in regions where *Axin2* expression is downregulated (Fig. 4F) and these spatial relationships resemble those of *Axin2* versus *L-fng* (Aulehla et al., 2003). These observations suggest that the oscillation of *nkd1* expression is regulated in a similar fashion to *L-fng*.

2.5. The oscillation of nkd1 expression is controlled by Hes7

To further confirm that the regulation of *nkd1* is under the control of the segmentation clock, via Notch signaling, we examined *nkd1* expression in the absence of Hes7 (Fig. 5A–C). In each of the Hes7-null embryos that we analyzed ($n=7$), the pattern of *nkd1* mRNA was similar. Strong expression was observed at the middle PSM, and weaker signals were observed in the remaining PSM. In comparison to wild-type embryos (Fig. 5D,E), it appeared that *nkd1* expression levels are upregulated and that its oscillatory patterns are arrested in Hes7 null-mice.

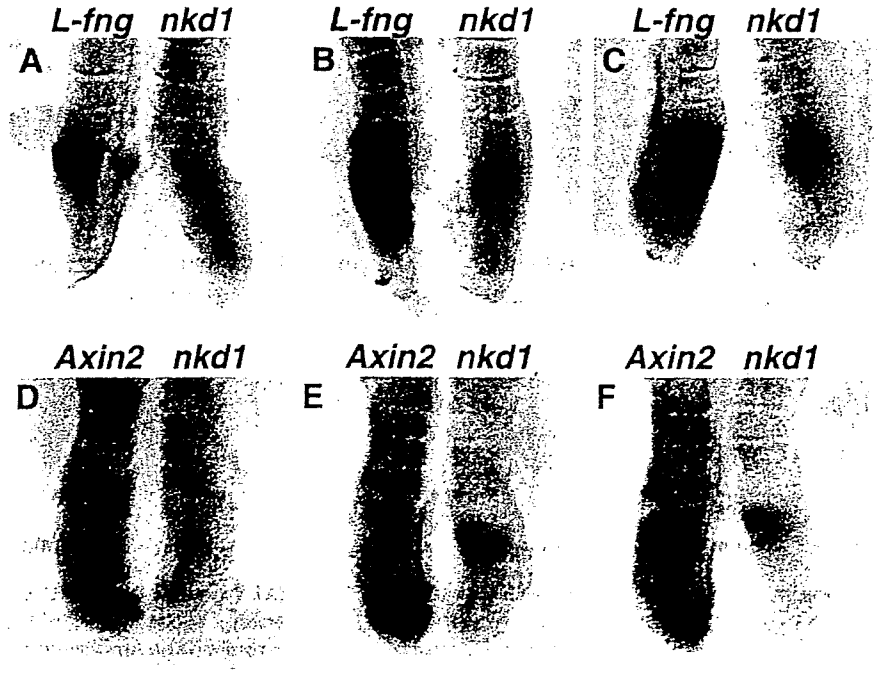

Fig. 4. Comparisons of the *nkd1* expression domains with the regions showing expression of other cyclic genes. (A–C) 11.5 dpc tail halves were stained with an *L-fng* probe (left) or an *nkd1* intron probe (right). The major expression domains overlapped with the exception of the anterior-most band of *L-fng* in B. (D–F) Embryo halves were stained with *Axin2* probe (left) or *nkd1* intron probe (right). The oscillatory phases of the expression patterns of *Axin2* and *nkd1* were found not to be synchronized.

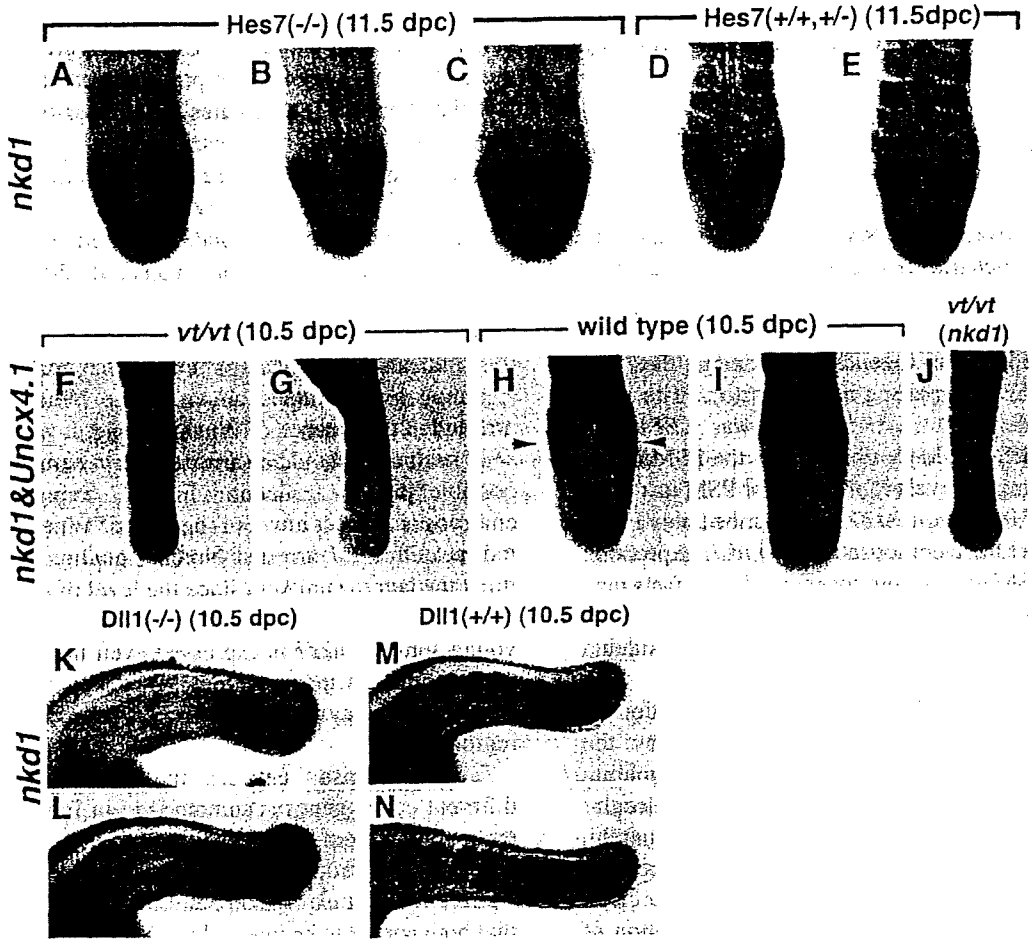

Fig. 5. *nkd1* oscillation is arrested in Hes7-null mice and its expression decreases in *vt/vt* mice but not in Dll1-null mice. (A–E) *nkd1* transcription was detected with an intron probe in either 11.5 dpc Hes7-null (A–C) or wild-type (D–E) littermate embryos. (F–I) *nkd1* expression in *vt/vt* and wild-type embryos was detected using an intron probe. *Uncx4.1* was used as an internal control. (J) *nkd1* probe alone was used in the *vt/vt* embryo. In the PSM of *vt/vt* embryos, *nkd1* mRNA is downregulated. The expression observed in the anterior PSM of wild-type embryo (arrowhead) corresponds to that of *nkd1* since *Uncx4.1* is expressed in the caudal portion of segmented somites. (K–N) *nkd1* expression in Dll1-null and wild-type embryos showing unaltered levels.

This suggests that the cyclic expression of *nkd1* depends on the negative regulation, either directly or indirectly, by the Hes7 transcription factor.

2.6. *nkd1* expression may be induced by Wnt signaling

In fly embryos lacking *Wg*, *nkd* transcription initiates normally but is not subsequently maintained (Zeng et al., 2000). In human colon tumors, initiated by activated Wnt/β-catenin signaling, *hnkd* (*NKD1*) expression is elevated and experimental reduction of β-catenin leads to a decrease in *nkd1* mRNA (Yan et al., 2001b). These findings suggest that *nkd1* expression and/or maintenance depends on Wnt signaling. To determine whether Wnt signals affect *nkd1* expression during somitogenesis, we investigated *nkd1* expression in the *Wnt3a* hypomorphic mutant *vestigial tail* (*vt*) embryo. The *Wnt3a* coding sequence in the *vt* mouse is intact but its expression is markedly reduced in the tailbud from 9.5 dpc because of the mutation in the *Wnt3a* regulatory region (Greco et al., 1996). In *vt/vt* embryos ($n=4$), *nkd1* transcription is greatly reduced in the middle PSM and tailbud regions (Fig. 5F,G and data not shown) whereas expression levels in the neural tube and newly formed somites are normal (Fig. 5J). The expression levels of *L-fng*, however, are not altered in *vt/vt* embryos (Aulehla et al., 2003), although no oscillation is observed in these mutants. In the PSM, we have shown that *nkd1* mRNA oscillations are produced by a similar mechanism to *L-fng*, via negative regulation by Hes7. However, the induction and/or maintenance of *nkd1* transcription may require a different signal from *L-fng*, and we speculate that this is probably provided via Wnt3a. To further confirm this possibility, we have analyzed *nkd1* expression in Dll1-null embryos. As shown in (Fig. 5K–N), no reduction was observed, emphasizing that *nkd1* expression itself is independent of Notch signaling. However, no clear oscillation was observed, which also suggests Notch-signal dependent oscillation of *nkd1*.

Taken together, our data suggest that a possible crosstalk between the Notch and Wnt signaling mechanisms and that

their reciprocal regulation might therefore be important for generating the cyclic waves required for refining somitogenesis.

3. Discussion

We have employed a cDNA subtraction method to isolate previously uncharacterized genes that either function downstream of Mesp2 and/or are specifically expressed in the PSM. We successfully isolated several genes that are putatively involved in somitogenesis, and among these we identified several Wnt-signaling related factors. The most abundant gene identified in our screen was *LEF1*, the expression of which is widely observed in the PSM but is detected at its strongest levels in the anterior PSM just prior to segment border formation. *nkd2* is transcribed only in the middle PSM but we have demonstrated that *nkd1* expression oscillates in the PSM during somitogenesis. These facts may indicate that Wnt signaling has an important role in somitogenesis, consistent with previous findings (Aulehla et al., 2003).

It is generally believed that the spatial reiteration of somites is based on the periodicity generated by the molecular segmentation clock. Several Notch-signaling related factors are known components of the molecular clock during somitogenesis (Pourquié, 2001). Additionally, mice lacking Notch-related factors fail to form regular somites, providing strong evidence that the molecular clock organized by Notch signaling is required for formation of the reiterated somite structure. One of the best characterized molecular clock components is Hes7 (Bessho et al., 2003), the upregulation of which depends on Notch signaling. Both the auto-inhibitory activity and instability of the Hes7 protein are responsible for its oscillatory expression properties. Recently, it has been reported that *Axin2* expression also oscillates and that Wnt3a is required for the oscillation of Notch signaling in the PSM, which lead to a postulated link between Wnt/β-catenin signaling and the segmentation clock (Aulehla et al., 2003). However, the mechanisms underlying the regulation of these oscillations have not yet been determined.

We have found that *nkd1* expression exhibits oscillation with a similar phase to *L-fng* during somitogenesis, and that this oscillation is arrested and the expression is upregulated in Hes7-null embryos. These observations strongly suggest that *nkd1* transcription is suppressed by Hes7, with concomitant generation of its cyclic expression. To determine whether Hes7 can bind to the *nkd1* enhancer directly, we attempted to find a Hes7 binding site upstream of the *nkd1* gene. However, some of the 5′ flanking sequences of *nkd1* are absent from the databases and we have not yet fully sequenced the genomic region and so far not found any E-box or N-box sites within the available sequences. Future enhancer analysis of *nkd1* will therefore be necessary to properly determine this possibility.

In the embryo of the Wnt3a hypomorphic mutant, *vestigial tail*, the expression of *nkd1* is greatly reduced in the PSM. This suggests the possibility that Wnt signaling (mediated by Wnt3a) regulates the expression of *nkd1* in the PSM. This would be consistent with previous reports showing that the maintenance of *Drosophila nkd* expression depends on Wg function (Zeng et al., 2000) and that activated Wnt signals induce elevated *hnkd* expression levels in human colon tumors (Yan et al., 2001b). However, as the level of *nkd1* expression is increased and the oscillation of *nkd1* is disrupted in the Hes7-null mutant, this indicates that *nkd1* is under the control of Notch signaling as mentioned above. Since Notch signaling is arrested in the absence of Wnt signaling, it was feasible that *nkd1* oscillation would be arrested in *vt/vt* embryos. It is also possible that the reduction in *nkd1* expression in *vt/vt* embryos is a direct effect of the lack of Wnt signaling or an indirect effect of arrested Notch signaling. However, we think the latter is unlikely since the level of *nkd1* expression is unaltered in Dll1-null embryos. In the neural tube or in young somites, *nkd1* is expressed even in the *vt/vt* mutant, which indicates that additional Wnt signals or possibly a different pathway may regulate *nkd1* transcription in these regions.

The comparison between the expression domains of different cyclic genes is summarized in Fig. 6A. The *nkd1* expression pattern is similar to that of both *hes7* and *L-fng*, but is different from *Axin2*. The reason why *Axin2* and *nkd1* exhibit different expression patterns, irrespective of the fact that both appear to be induced by Wnt signaling, is currently unknown. One possibility is that *nkd1*, but not *Axin2*, oscillation is regulated by Notch signaling, which results in synchronization of *nkd1* oscillation with Notch signaling. In other words, the initial induction of *nkd1* might be induced by Wnt signaling but its regulation is under the control of Notch signaling. However, the expression patterns of Notch-related genes and *Axin2* are not completely mutually exclusive. They appear to be alternate in the tailbud region but they do align in the anterior PSM where *Mesp2* is expressed. Wnt3a appears to induce the expression of *Axin2* directly, but *Wnt3a* mRNA is detected only in the tailbud (Aulehla et al., 2003). Considering that Axin2 is expressed as a detectable band in the anterior PSM and that its expression is altered in Mesp2-null embryos, the expression pattern of *Axin2* may be regulated by Mesp2 in the anterior PSM. The direct targets of Mesp2 have not yet been characterized but many genes that are expressed in the anterior PSM are affected (downregulated or anteriorly expanded) by Mesp2, including *Notch1*, *Notch2*, *Fgfr1*, *Dll1*, *EphA4*, *Papc*, *Cer1* and *L-fng* (Saga et al., 1997; Takahashi et al., 2000; Nomura-Kitabayashi et al., 2002). Among them, EphA4 is implicated in segment border formation and ectodermal signaling is also required for *EphA4* induction (Schmidt et al., 2001), which may suggest that downstream genes of Wnt signal from the ectoderm might interact with Mesp2 to induce *EphA4*. *nkd1* is not

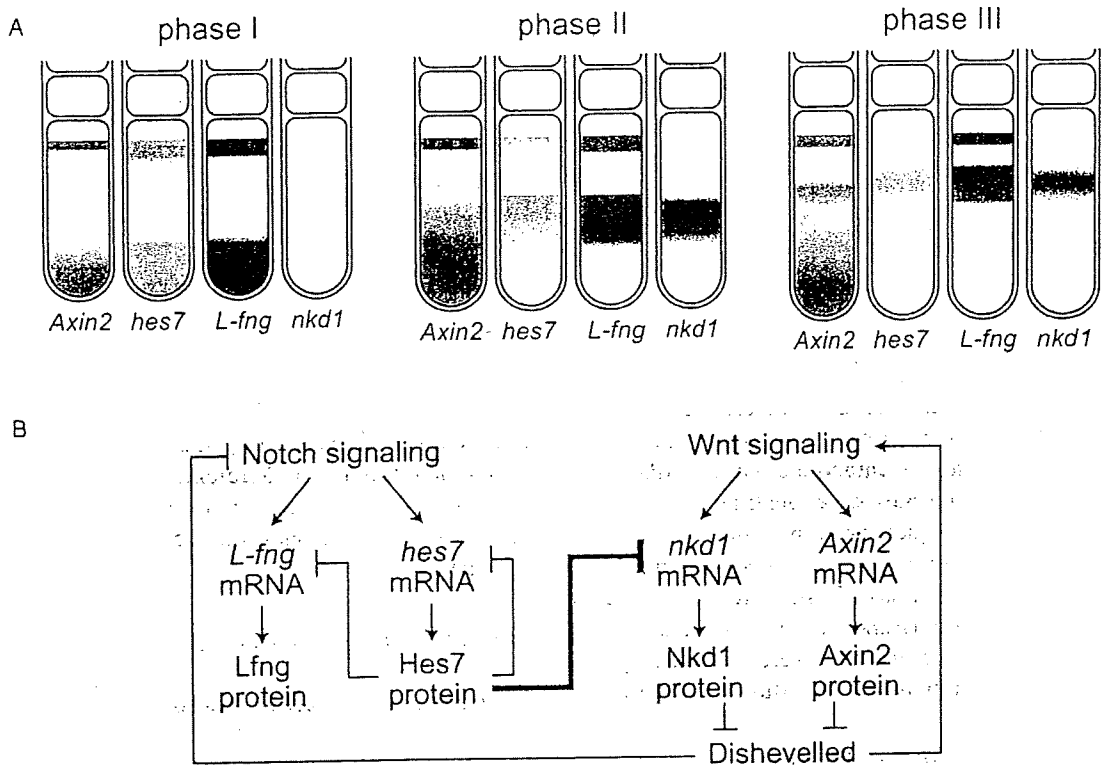

Fig. 6. (A) A schematic diagram of the expression patterns of oscillatory genes in the PSM of 11.5 dpc embryos. PhaseI: *Axin2*, *hes7* and *L-fng* show similar expression patterns in the tailbud and anterior PSM. *nkd1* transcription is greatly downregulated in this phase. PhaseII: The expression domain of *Axin2* is more extensive in the tailbud region. *hes7*, *L-fng* and *nkd1* are all expressed in the same region of the middle PSM, whereas *nkd1* is not detected in the anterior PSM in a band-like pattern. PhaseIII: *Axin2* expression is downregulated in the middle PSM. Around S-1, the expression of all four genes overlaps. (B) Possible interactions between Notch and Wnt signaling. Our findings are integrated into the previously proposed schemes of Bessho et al. (2003) and Aulehla et al. (2003). We propose that Wnt signaling may be regulated by Notch signals via the transcriptional regulation of *nkd1* by Hes7. It has been reported previously that Wnt signaling may regulate Notch signaling via NICD inhibition by Dishevelled (Axelrod et al., 1996).

expressed in the anterior PSM and its expression is regulated by Hes7, but not by Mesp2 (data not shown). There may be different gene regulatory mechanisms along the AP axis in the PSM, where the cyclic expression in the posterior PSM must be regulated by a clock mechanism, but expression in the anterior PSM may also be regulated by a different mechanism under the control of Mesp2. The link between these two mechanisms is currently unknown but the clock mechanism which is operated by both Wnt and Notch signaling may affect Mesp2 regulation.

nkd is a *Drosophila* segment polarity gene that encodes an antagonist of the Wnt signal, Wingless. It is known that mouse Nkd1 directly binds to Dishevelled (Dvl) (Wharton et al., 2001) and that Nkd1 antagonizes Wnt signaling in both *Xenopus* (Yan et al., 2001a) and *Drosophila* (Wharton et al., 2001) embryos. Thus, it is possible that the Nkd1 protein also functions as an antagonist of Wnt signaling in the PSM. Of great interest, therefore, is the exact function of Nkd1 during somitogenesis. Using luciferase reporter assays, it has previously been demonstrated that *Axin2* is directly upregulated by Wnt/β-catenin signaling (Aulehla et al., 2003). One possibility, therefore, for the function of Nkd1 is that, in mouse, it suppresses the transcription of *Axin2* by antagonizing the Wnt signals, and hence, Nkd1 oscillations may contribute to the oscillatory expression of *Axin2*. To further address this question, it will be necessary to analyze the distribution of the Nkd1 protein and examine whether it has a sufficiently high turnover to generate such oscillatory expression patterns. However, both Axin and Nkd1 have been demonstrated to bind Dvl via its PDZ domain (Li et al., 1999; Seidensticker and Behrens, 2000; Yan et al., 2001a; Wharton et al., 2001). Hence, if Axin2 can bind Dvl with a similar affinity as Axin, it may compete with Nkd1 for Dvl binding to initiate distinct functions. Alternatively, they may work co-operatively to suppress Dvl. The binding to Dvl not only affects Wnt signaling but also may affect Notch signaling since it has already been shown to bind the processed form of Notch receptor (NICD) (Axelrod et al., 1996). It has also been reported that Dvl1/Dvl2 double knockout embryos exhibit defects in somite segmentation (Hamblet et al., 2002), which may suggest that regulation of Wnt signaling via Axin2 and /or Nkd1 is involved in segmental patterning. The link between Wnt and Notch signaling remains one of the central unsolved mechanisms underlying both the generation and regulation of the segmentation clock. Since *nkd1* oscillation is

disrupted in Hes7-null mutants, there may be a negative feed-back loop between the Notch and Wnt signaling pathways and it is likely that their interaction is essential for the establishment of the molecular clock required for accurate somitogenesis (Fig. 6B).

4. Experimental procedures

4.1. Experimental animals

Heterozygous Mesp2-mutant (*Mesp2*$^{+/-}$) mice were intercrossed to obtain either homozygous, heterozygous or wild-type embryos in the same litter. The appearance of vaginal plugs was designated as embryonic day 0.5 (dpc). Homozygous Mesp2-null embryos were identified by a no segmentation phenotype, as described previously (Saga et al., 1997). Hes7-knockout mice and Dll1-knockout mice were kindly provided by Yasumasa Bessho (Kyoto Univ. Japan) and Achime Gosller (Hanover Univ. Germany), respectively. Samples of *vt/vt* embryos were provided by Shinji Takada (National Institute for Basic Biology, Japan).

4.2. Preparation of subtractive cDNA libraries

As shown in Fig. 1, total RNA isolates were prepared from two pieces of the dissected portions of either wild-type (WP: PSM of wild-type and WS: somite region of wild-type) or homozygous (HPS: PSM of Mesp2-null) 11.5 dpc embryos using Isogen (Nippon Gene, Japan). We utilized the subtractive hybridization method of Kaneko-Ishino et al. (1995) with slight modifications. Briefly, to generate tester cDNAs for subtraction, cDNAs were synthesized and amplified with the Smart cDNA Amplification Kit (Clontech, USA), whereas the driver cDNAs were generated using a cDNA Synthesis Kit (TaKaRa, Japan). Amplification of driver cDNAs was performed using a ligated linker (P-linker). A biotinylated P-primer, complementary to the P-linker, was used for the subsequent PCR (Kaneko-Ishino et al., 1995).

PCR primer 5′-AAGCAGTGGTAACAACGCAGAGT-3′.
P-linker 5′-GATTACTCGAGACTAATATC-3′;
5′-pGATATTAGTCTCGAGTA-3′.

We constructed two libraries; one generated by subtraction between [WP] (tester) and [WS] (driver) to enrich for PSM genes, and a second synthesized by subtraction between [WP] (tester) and [HPS] (driver) to enrich for possible Mesp2 downstream genes. Tester cDNA samples (60 ng) were hybridized to biotinylated driver cDNAs (1.2 μg) (the ratio was increased to 1:100 in the case of the second and third subtractions). After ethanol precipitation, total cDNAs were subjected to absorption by 4 mg of Dynabeads M-280 conjugated to streptavidin (Dynal). The remaining cDNAs were amplified by PCR. One half of each sample was used for the subsequent subtraction steps, and the cDNA isolates that were obtained after three consecutive subtractions and PCR amplifications were cloned into the pCRII vector using a TA Cloning Kit (Invitrogen). We designated these subtractive libraries as the PTS library for [WP] and [WS], and as the ST library for [WP] and [HPS].

4.3. Sequencing and computer analysis

cDNA clones that were randomly selected from both of the subtractive libraries that we generated, 406 and 636 clones from PTS and ST, respectively, were partially sequenced and analyzed using the BLAST program through the National Library of Medicine and Celera databases. Only novel clones were further screened by ISH. The numbers of selected clones were 251 and 280, for PTS and ST, respectively.

4.4. Screening by in situ hybridization

The basic method used for whole mount ISH has been described previously by our laboratory (Saga et al., 1996), although for this study automated ISH was employed (InsituPro, M&S Instruments Trading Inc. Japan). The tail regions, containing both somite and PSM of 11.5 dpc embryos, were used in these analyses. RNA probes were generated by transcription, with either T7 RNA polymerase or SP6 RNA polymerase, of template DNAs prepared by PCR using M13 specific sites within the vector. M13 reverse primer: 5′-CAGGAAACAGCTATGAC-3′; M13 forward primer: 5′-GTAAAACGACGGCCAG-3′.

4.5. Whole-mount in situ hybridization probes

A BamHI-PstI 429 bp fragment of *nkd1* cDNA was used as an *nkd1* exon probe. As *nkd1* intron probes, we utilized a mixture of two genomic fragments; the XbaI 1.3 kb fragment in intron 4 and the NcoI 1.4 kb fragment in intron 6. For *Axin2* hybridization, we amplified a 1360 bp PCR fragment from the coding region of this gene from a PSM cDNA library (Ohara et al., 2002) using the forward primer 5′-GTCTGGAGGAGCGGCTGCAGCAGATCCG-3′ and reverse primer 5′-CAAGGCTCAGTCGATCCTCTC-CACTTTGC-3′.

4.6. In vitro explant cultures

In vitro explant culture was performed as previously described (Takahashi et al., 2000). The tail regions of ICR embryos (11.5 dpc) were bisected at the midline with either a tungsten or ground sewing needle. One half was fixed immediately and the other was cultured for either 60 or 120 min. After culturing, specimens were fixed and used for subsequent ISH analysis.

Acknowledgements

We thank Yasumasa Bessho for providing the Hes-7 knockout mouse and Shinji Takada for donating the vt/vt embryos. We also thank Mariko Ikumi, Izumi Uehara and Eriko Ikeno for general technical assistance. This work was supported by Grants-in-Aid for Science Research on Priority Areas (B), the Organized Research Combination System and National BioResource Project of the Ministry of Education, Culture, Sports, Science and Technology, Japan.

References

Aulehla, A., Wehrle, C., Brand-Saberi, B., Kemler, R., Gossler, A., Kanzler, B., Herrmann, B.G., 2003. Wnt3a plays a major role in the segmentation clock controlling somitogenesis. Dev. Cell 4, 395–406.

Axelrod, J.D., Matsuno, K., Artavanis-Tsakonas, S., Perrimon, N., 1996. Interaction between Wingless and Notch signaling pathways mediated by dishevelled. Science 271, 1826–1832.

Behrens, J., Jerchow, B., Würtele, M., Grimm, J., Asbrand, C., Wirtz, R., et al., 1998. Functional interaction of an axin homolog, conductin, with β-catenin, APC, and GSK3β. Science 280, 596–599.

Bessho, Y., Sakata, R., Komatsu, S., Shiota, K., Yamada, S., Kageyama, R., 2001. Dynamic expression and essential functions of Hes7 in somite segmentation. Genes Dev. 15, 2642–2647.

Bessho, Y., Hirata, H., Masamizu, Y., Kageyama, R., 2003. Periodic repression by the bHLH factor Hes7 is an essential mechanism for the somite segmentation clock. Genes Dev. 17, 1451–1456.

Dubrulle, J., McGrew, M.J., Pourquie, O., 2001. FGF signaling controls somite boundary position and regulates segmentation clock control of spatiotemporal Hox gene activation. Cell 106, 219–232.

Greco, T.L., Takada, S., Newhouse, M.M., McMahon, A.P., Camper, S.A., 1996. Analysis of the vestigial tail mutation demonstrates that Wnt-3a gene dosage regulates mouse axial development. Genes Dev. 10, 313–324.

Hamblet, N.S., Lijam, N., Ruiz-Lozano, P., Wang, J., Yang, Y., Luo, Z., et al., 2002. Dishevelled 2 is essential for cardiac outflow tract development, somite segmentation and neural tube closure. Development 129, 5827–5838.

Hsu, S., Galceran, J., Grosschedl, R., 1998. Modulation of transcriptional regulation by LEF-1 in response to Wnt-1 signaling and association with β-catenin. Mol. Cell Biol. 18, 4807–4818.

Kaneko-Ishino, T., Kuroiwa, Y., Miyoshi, N., Kohda, T., Suzuki, R., Yokoyama, M., et al., 1995. Peg1/Mest imprinted gene on chromosome 6 identified by cDNA subtraction hybridization. Nature Genet. 11, 52–60.

Li, L., Yuan, H., Weaver, C.D., Mao, J., Farr III., G.H., Sussman, D.J., et al., 1999. Axin and Frat1 interact with dvl and GSK, bridging Dvl to GSK in Wnt-mediated regulation of LEF-1. Eur. Mol. Biol. Org. J. 18, 4233–4240.

Liu, Y., Jiang, H., Crawford, H.C., Hogan, B.L., 2003. Role for ETS domain transcription factors Pea3/Erm in mouse lung development. Dev. Biol. 261, 10–24.

Nomura-Kitabayashi, A., Takahashi, Y., Kitajima, S., Inoue, T., Takeda, H., Saga, Y., 2002. Hypomorphic Mesp allele distinguishes establishment of rostrocaudal polarity and segment border formation in somitogenesis. Development 129, 2473–2481.

Ohara, O., Nagase, T., Mitsui, G., Kohga, H., Kikuno, R., Hiraoka, S., et al., 2002. Characterization of size-fractionated cDNA libraries generated by the in vitro recombination-assisted method. DNA Res. 9, 47–57.

Palmeirim, I., Henrique, D., Ish-Horowicz, D., Pourquié, O., 1997. Avian hairy gene expression identifies a molecular clock linked to vertebrate segmentation and somitogenesis. Cell 91, 639–648.

Porfiri, E., Rubinfeld, B., Albert, I., Hovanes, K., Waterman, M., Polakis, P., 1997. Induction of a β-catenin-LEF-1 complex by wnt-1 and transforming mutants of β-catenin. Oncogene 15, 2833–2839.

Pourquié, O., 2001. Vertebrate somitogenesis. Annu. Rev. Cell Dev. Biol. 17, 311–350.

Rasmussen, J.T., Deardorff, M.A., Tan, C., Rao, M.S., Vetter, M.L., 2001. Regulation of eye development by frizzled signaling in Xenopus. Proc. Natl Acad. Sci. USA 98, 3861–3866.

Ristevski, S., Tam, P.P., Hertzog, P.J., Kola, I., 2002. Ets2 is expressed during morphogenesis of the somite and limb in the mouse embryo. Mech Dev. 116, 165–168.

Saga, Y., Hata, N., Kobayashi, S., Magnuson, T., Seldin, M., Taketo, M.M., 1996. MesP1: a novel basic helix-loop-helix protein expressed in the nascent mesodermal cells during mouse gastrulation. Development 122, 2769–2778.

Saga, Y., Hata, N., Koseki, H., Taketo, M.M., 1997. Mesp2: a novel mouse gene expressed in the presegmented mesoderm and essential for segmentation initiation. Genes Dev. 11, 1827–1839.

Sawada, A., Shinya, M., Jiang, Y.J., Kawakami, A., Kuroiwa, A., Takeda, H., 2001. Fgf/MAPK signalling is a crucial positional cue in somite boundary formation. Development 128, 4873–4880.

Schmidt, C., Christ, B., Maden, M., Brand-Saberi, B., Patel, K., 2001. Regulation of Epha4 expression in paraxial and lateral plate mesoderm by ectoderm-derived signals. Dev. Dyn. 220, 377–386.

Seidensticker, M.J., Behrens, J., 2000. Biochemical interactions in the wnt pathway. Biochem. Biophys. Acta 1495, 168–182.

Takada, S., Stark, K.L., Shea, M.J., Vassileva, G., McMahon, J.A., McMahon, A.P., 1994. Wnt-3a regulates somite and tailbud formation in the mouse embryo. Genes Dev. 8, 174–189.

Takahashi, Y., Koizumi, K., Takagi, A., Kitajima, S., Inoue, T., Koseki, H., Saga, Y., 2000. Mesp2 initiates somite segmentation through the Notch signalling pathway. Nature Genet. 25, 390–396.

Takahashi, Y., Inoue, T., Gossler, A., Saga, Y., 2003. Feedback loops comprising Dll1, Dll3 and Mesp2, and differential involvement of Psen1 are essential for rostrocaudal patterning of somites. Development 18, 4259–4268.

Tan, C., Deardorff, M.A., Saint-Jeannet, J.P., Yang, J., Arzoumanian, A., Klein, P.S., 2001. Kermit, a frizzeled interacting protein, regulates frizzeled 3 signaling in neural crest development. Development 128, 3665–3674.

Wharton Jr., K.A., Zimmermann, G., Rousset, R., Scott, M.P., 2001. Vertebrate proteins related to Drosophila Naked Cuticle bind Dishevelled and antagonize Wnt signaling. Dev. Biol. 234, 93–106.

Yamamoto, H., Flannery, M.L., Kupriyanov, S., Pearce, J., McKercher, S.R., Henkel, G.W., et al., 1998. Defective trophoblast function in mice with a targeted mutation of Ets2. Genes Dev. 12, 1315–1326.

Yan, D., Wallingford, J.B., Sun, T.Q., Nelson, A.M., Sakanaka, C., Reinhard, C., et al., 2001a. Cell autonomous regulation of multiple Dishevelled-dependent pathways by mammalian Nkd. Proc. Natl Acad. Sci. USA 98, 3802–3807.

Yan, D., Wiesmann, M., Rohan, M., Chan, V., Jefferson, A.B., Guo, L., et al., 2001b. Elevated expression of axin2 and hnkd mRNA provides evidence that Wnt/β-catenin signaling is activated in human colon tumors. Proc. Natl Acad. Sci. USA 98, 14973–14978.

Zeng, W., Wharton Jr., K.A., Mack, J.A., Wang, K., Gadbaw, M., Suyama, K., et al., 2000. Naked cuticle encodes an inducible antagonist of Wnt signalling. Nature 403, 789–795.

Toxicologic Pathology, 32(Suppl. 2):12–16, 2004

ISSN: 0192-6233 print / 1533-1601 online
DOI: 10.1080/01926230490451725

Mechanism of Benzene-Induced Hematotoxicity and Leukemogenicity: Current Review with Implication of Microarray Analyses

YOKO HIRABAYASHI,[1] BYUNG-IL YOON,[1,2] GUANG-XUN LI,[1] JUN KANNO,[1] AND TOHRU INOUE[3]

[1]*Division of Cellular and Molecular Toxicology, National Institute of Health Sciences, Tokyo 158-8501, Japan*
[2]*Department of Veterinary Medicine, Kangwon National University, Kangwon 200-701, Republic of Korea, Seoul National University, Seoul 151-742, Republic of Korea, and*
[3]*Biological Safety and Research Center, National Institute of Health Sciences, Tokyo 158-8501, Japan*

ABSTRACT

Benzene is a potent human leukemogen but the mechanism underlying benzene-induced leukemia remains an enigma due to a number of questions regarding the requirement of extraordinarily long exposure, a relatively low incidence of leukemia for genotoxicity of metabolites and a narrow dose range for leukemogenicity over marrow aplasia (overdoses tend to result in marrow aplasia). Moreover, there were previous controversies as to whether the cell cycle is upregulated or suppressed by the benzene exposure. Subsequently, it was found that the cell cycle is suppressed, but how leukemia develops under such suppression of hemopoiesis remains to be clarified. These questions were fortunately resolved with much effort. Benzene exposure was found to induce the expression of p21, an interlocking counterdevice for cell cycle: due to *p53* upregulation, thereby inducing the immediate suppression of the kinetics of hemopoietic progenitors followed by the prominent suppression of hemopoiesis. Intermittent benzene exposure (i.e., cessation of exposure during weekends, for example) allowed an immediate recovery from marrow suppression after terminating exposure, which induced continuous oscillatory changes in marrow hemopoiesis. Benzene-induced leukemia was chiefly due to such an oscillatory change in hemopoiesis, which epigenetically developed leukemia more than 1 year later. The mechanisms of benzene-induced leukemogenicity seem to differ between wild-type mice and mice lacking *p53*. For *p53* knockout mice, DNA damage such as weak mutagenicity or chromosomal damage was retained, and such damage induced consequent activation of proto-oncogenes and related genes, which led cells to undergo further neoplastic changes. In contrast, for wild-type mice carrying the *p53* gene, a marked oscillatory change in the cell cycle of the stem cell compartment seems to be important. Compatible and discriminative gene expression profiling between the *p53* knockout mice and wild-type mice was observed after benzene exposure by microarray analyses.

Keywords. Benzene; hematotoxicity; leukemogenicity; gene chip array; BUUV method; *p53*-KO; AhR-KO; hemopoietic progenitor cells.

INTRODUCTION

The mechanism of benzene-induced leukemia had long been an enigma until recently, when the unique cell kinetics of stem/progenitor cells during benzene exposure was elucidated. Leukemia induction by benzene inhalation was first reported in 1897, when Le Noire described multiple cases of leukemia among Parisian cobblers (Le Noir and Claude, 1897). However, the experimental induction of leukemia by benzene exposure was first reported about 20 years ago by Snyder et al. (1980) and our group (Cronkite et al., 1984, 1989). Recently, we demonstrated marked oscillatory changes in peripheral blood and bone marrow (BM)[1] cellularities during and following benzene inhalation, preceding the development of leukemia by about 1 year (Hirabayashi et al., 1998; Kawasaki et al., 2001; Yoon et al., 2001).

Benzene-induced leukemia is unique in that it has been associated only with a weak mutagenicity in the benzene metabolites, phenol and hydroquinone. Another interesting observation is the controversial experimental data concerning the level of actively cycling hematopoietic cells following benzene exposure. While all researchers observed a decrease in peripheral blood and BM cellularities, some observed a suppression of the cell cycle of BM, as measured by tritiated thymidine incorporation (Moeschlin and Speck, 1967), whereas others observed a marked increase in the number of cycling stem/progenitor cells in BM and peripheral blood (Table 1). Careful analysis of these apparently conflicting data revealed an enhancement of the cell cycle occurring at least 2 hours after the termination of benzene exposure. Thus, the higher tritiated thymidine incorporation documented by Cronkite et al. (1982) 18 hours after the termination of benzene exposure probably reflects a recovery phase. Based on these findings, we conducted a series of studies since 1997 to elucidate the leukemogenic effect of benzene in wild-type mice.

The *p53*-knockout (KO) mouse (Tsukada et al., 1993) showed further unique characteristics of benzene-induced leukemia. Using *p53*-KO mouse, we confirmed that benzene has a moderate genotoxic effect, as measured by the micronucleus test performed 4 weeks after the initiation of benzene inhalation (Kawasaki et al., 2001; Li et al., 2003). Moreover, *p53*-deficient mice manifest increased susceptibility to

Address correspondence to: Tohru Inoue, Center for Biological Safety and Research, National Institute of Health Sciences, 1-18-1 Kamiyohga, Setagayaku, Tokyo 158-8501, Japan; e-mail: tohru@nihs.go.jp

[1]Abbreviations: BM, bone marrow; KO, knockout; UV, ultraviolet; BUUV, incorporation of bromodeoxyuridine followed by ultraviolet-light cytocide to evaluate the hemopoietic stem/progenitor cell kinetics in vivo; AhR, aryl hydrocarbon receptor; $AhR^{+/+}$, AhR wild-type; $AhR^{+/-}$, AhR heterozygous-deficient; $AhR^{-/-}$, AhR homozygous-deficient; CFU-GM, granulo-macrophage colony forming unit; CYP, cytochrome P450; FGF, fibroblast growth factor; TGF, tumor growth factor; I.V., intravenous; I.P., intraperitoneal; aft, after; dur, during; expos, exposure.

TABLE 1.—Summary of the results the hemopoietic stem/progenitor cell kinetics during and after benzene exposure by tritiated thymidine (^{3}H-TdR) cytocide assay.

				Evaluation cell and assay methods					
		Cellularity		BM cells			CFU		
Year	Reference	Blood	BM	Kinetics	Labeling*,[1]	Label point	Kinetics	Labeling	Label point
1967	Moeschlin and Speck	↓	↓	↓	In vivo	At pancytopenia	—	—	—
1979	Irons et al.	↓	↓	↑	In vivo[2]	6 days aft. expos-IP	—	—	—
1982	Cronkite et al.	↓	↓	—	—	—	↑	In vitro	18 h aft. expos.
1998	Lee et al.	↓	↓	↓	In vivo[3]	30 min aft. single IP	—	—	—
		↓	↓	↓	In vitro	Dur. and aft. expos.	—	—	—
1997	Farris et al.	↓	↓	→↓	In vivo[4]	Soon aft. expos.	↑	In vitro	2 h aft. expos.

1. ^{3}H-TdR was injected intravenous (IV) at in vivo labeling except indications.
2. ^{3}H-TdR was injected intraperitoneal (IP) 6 days after cessation of benzene.
3. Benzene was treated single IP, and ^{3}H-TdR label was starting 30 minutes after benzene treatment.
4. Instead of ^{3}H-TdR, BrdUrd was used for assay.

benzene-induced leukemogenicity (Kawasaki et al., 2001). Similar findings with regard to increased leukemogenicity following benzene exposure have been documented by French et al. of the National Institute of Environmental Health Sciences (French et al., 2001). Contrary to the result in *p53*-KO mice, benzene-induced leukemia had not been detected in earlier studies in wild-type mice because its manifestations had been masked either by pancytopenia due to severe myelosuppression or by the use of a benzene dose too low to induce pancytopenia or leukemia (Kawasaki et al., 2001). Aryl hydrocarbon receptor (AhR)-KO mice (Mimura et al., 1997) also elucidated the characteristic underlying mechanism of benzene-induced hematotoxicity (Yoon et al., 2002).

In the mechanism underlying benzene toxicity in BM tissue analyzed using a microarray system, various signaling pathways have been suggested to be implicated including cell cycle regulation, DNA-damage/repair-related genes, oxidative-stress-related genes, growth-factor-related genes, oncogenes, and hemopoiesis-related genes in general (Yoon et al., 2003).

OSCILLATORY CHANGES IN BONE MARROW CELLULARITY IN WILD-TYPE MICE

BM cellularity decreases markedly during benzene inhalation but recovers rapidly following the termination of benzene exposure (Yoon et al., 2001). The oscillatory nature of the resultant curve is comparable to the response reported by Cronkite et al. (1984, 1989), and suggests that benzene does not only induce BM cell suppression but also activates cell-cycle-regulating genes, resulting in compensatory myelopoiesis.

We used the BUUV (bromodeoxyuridine + UV exposure) method to study stem/progenitor cell kinetics during or after benzene exposure (Hirabayashi et al., 1998; Yoon et al., 2001). Using this method, we were able to measure the labeling rate, cycling fraction of clonogenic progenitor cells, and other cell cycle parameters. Interestingly, the cycling fraction of stem/progenitor cells was found not to turn into active hematopoiesis but to remain low during benzene inhalation. Furthermore, rapid recovery was observed after benzene inhalation was terminated (Figure 1). However, although the exact mechanism of this phenomenon is not yet known, we found the evidence that the cycling fraction depression may be mediated in part by the suppression of stem/progenitor cell cycling per se, owing to the *p53*-dependent upregulation of p21 (Yoon et al., 2001). Thus, the mechanism of benzene-induced leukemia in the wild-type mice may be due to continuous oscillatory changes in hemopoiesis during and after the benzene exposure, which leads to genetic instability followed by the consequent epigenetic leukemogenicity.

p53-DEFICIENT MICE DEVELOP LEUKEMIA BY DIFFERENT MECHANISMS

Leukemogenicity induced in *p53*-KO mice, because of the lack of the *p53* gene, results in the noninduction of p21 expression even during the benzene exposure, with subsequent insufficient DNA repair and accumulation of DNA damage. These pathways are shown in Figure 2 for benzene-induced possible toxicological changes in both wild-type and *p53*-KO mice. In *p53*-KO mice, cell cycle suppression, DNA repair, and apoptosis of damaged cells, which, in general, occur in the wild-type mice after benzene exposure, are all suppressed. This is much more likely genotoxic leukemogenesis, in which reactive oxygen species, dysfunction of topoisomerase, and covalent binding of adduct formation to DNA,

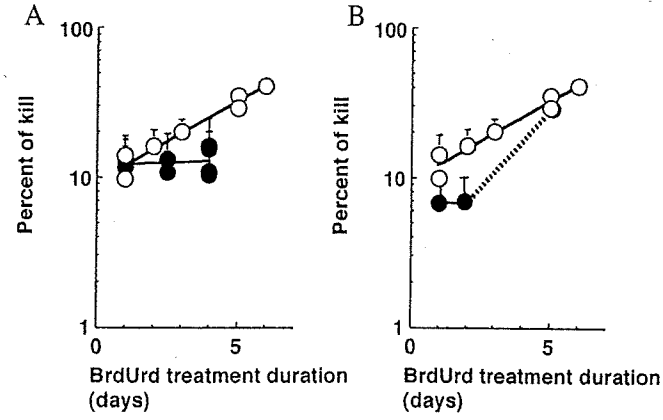

FIGURE 1.—Hemopoietic progenitor cell (CFU-GM) kinetics during (A) and after (B) benzene inhalation. Open circle: sham; Closed circle: during or after inhalation of 300 ppm benzene, 6 h/day, 5 days/week ×2 weeks. (A) For the benzene-treated group, all the mice were sacrificed just after the 5th day of the 2nd week of benzene-inhalation. The osmotic minipump filled with BrdUrd was implanted into donor mice day(s) before sacrificing as indicated on the abscissa. (B) For the benzene-treated group, the BrdUrd-pump was implanted into donor mice after the 5th day of the 2nd week of benzene-inhalation and sacrificed on the day as indicated on the abscissa. Each point represents at least 2 mice as a donor for the CFU-GM assay, and colony assays were performed in triplicate.

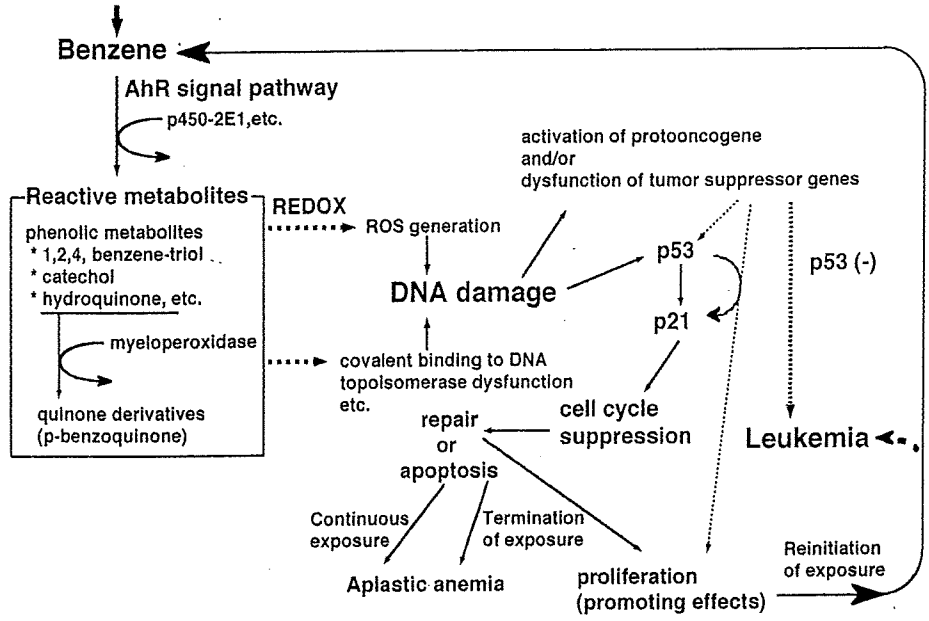

FIGURE 2.—Benzene metabolism and possible mechanism of benzene-induced leukemogenesis.

all synergistically participate in further leukemogenic development without repairing the system (see Figure 2). Thus, leukemogenicity seems to be clearly different between the mice carrying wild-type *p53* and the mice lacking *p53* (Yoon et al., 2001; Hirabayashi et al., 2002).

ARYLHYDROCARBON-RECEPTOR-MEDIATED BENZENE METABOLISM

We investigated the involvement of the aryl hydrocarbon receptor (AhR), a ligand-activated basic helix-loop-helix transcription factor, in hematotoxicity using AhR wild-type ($AhR^{+/+}$), heterozygous-KO ($AhR^{+/-}$) and homozygous-KO ($AhR^{-/-}$) male mice (Mimura et al., 1997; Yoon et al., 2002). Following a 2-week inhalation of benzene at 300 ppm, we evaluated the changes in cellularity of the peripheral blood and BM, and the levels of granulocyte-macrophage colony-forming units (CFU-GM) in the BM (Figure 3). The expression of the cyclin-dependent kinase inhibitor, p21, in BM cells and cytochrome P450 (CYP) 2E1 in hepatic tissues were evaluated by Western blot analysis after benzene exposure. Our results clearly showed that $AhR^{-/-}$ mice are much more resistant to the benzene-induced hematotoxicity than $AhR^{+/+}$ wild-type mice. No changes in p21 expression level by BM cells were detected in $AhR^{-/-}$ mice, whereas a marked up-regulation of p21 expression by BM cells was observed in $AhR^{+/+}$ mice. This finding is a further proof of the resistance of $AhR^{-/-}$ mice to benzene-induced hematotoxicity. The benzene resistance of $AhR^{-/-}$ mice was abrogated by exposure to a combination of 2 major metabolites, phenol and hydroquinone, strongly supporting the notion that AhR participates in benzene metabolism. CYP species involved in such metabolism are under investigation. The results obtained imply that pollutants that react with AhR confer marked susceptibility to benzene-induced hematotoxicity.

IMPLICATION OF MICROARRAY ANALYSIS

In the mechanism underlying benzene toxicity in BM tissue, various signaling pathways have been suggested to be implicated including metabolism, genotoxicity, cell cycle regulation, and apoptosis (Table 2). Our microarray analysis

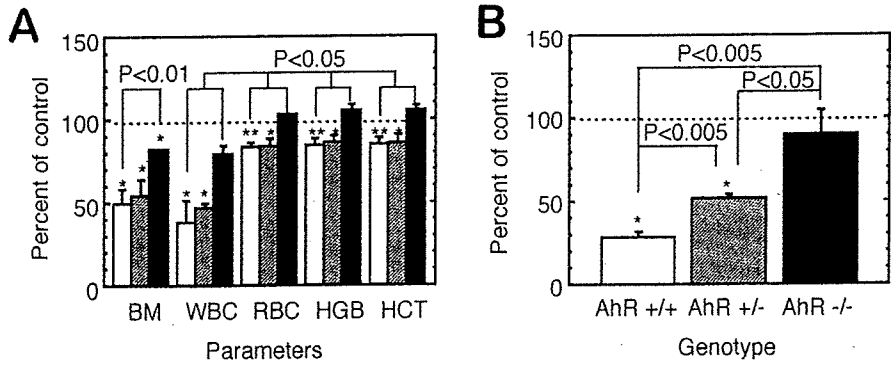

FIGURE 3.—Changes in peripheral blood parameters and BM cellularity (A) and CFU-GM per 2 femurs (B) in the AhR wild-type ($AhR^{+/+}$:open bar), heterozygous-KO ($AhR^{+/-}$:shaded bar) and homozygous-KO mice ($AhR^{-/-}$:closed bar) exposed to 300 ppm benzene for 2 weeks. The mean BM cellularities for the $AhR^{+/+}$, $AhR^{+/-}$, and $AhR^{-/-}$ mice were 4.8, 5.6, and 4.8 $\times$ 10^7/2 femurs, respectively, and the mean numbers of CFU-GM's per 8 $\times$ 10^4 BM cells was 79, 78, and 72, respectively. *, **: Significantly different from each corresponding control group at $p < 0.05$ and $p < 0.01$, respectively.

TABLE 2.—Reported genes whose expression changed during and/or after benzene inhalation.

Category	Gene name	Reference
Metabolic enzyme	CYP 2E1	Zhang et al., 2002
	Myeloperoxidase	Schattenberg et al., 1994
Cell cycle	*p53*	Boley et al., 2002
	p21 (waf 1)	
	Cyclin G	
	Gadd 45	
Apoptosis	Bax-alpha	Boley et al., 2002
Oncogene	c-fos	Ho and Witz, 1997

elucidated the up- or downregulation of genes functioning after 2-week exposure to 300 ppm benzene (Table 3): First, among cell-cycle-related genes, in addition to *p53* and p21 which are known to be upregulated to various extents depending upon the time course and the detection methods, Rb-related genes, such as the Rb-related protein p130 and the Rb-binding protein p48 are significantly upregulated; furthermore, elongation factor 1-delta shows a high expression level associated with the G2/M cell cycle checkpoint; vice versa, a significant downregulation of cyclin D1 and BimB is also recognized. Less significant changes in expression of cyclin G and Gadd45 are noted as previously reported. Second, among DNA-damage/repair-related genes, those encoding ADP-ribosylation factor-like protein 1 and Rad51 are significantly upregulated. The altered expression of other genes in the same category such as Metaxin, ERCC-3, and the DTR111 precursor are also noted, although p-values are not statistically significant. Third, among oxidative-stress-related genes, mitogen-activated protein kinase 2, which responds primarily to stress and inflammatory stimuli, is significantly upregulated, and the known typical ROS absorber genes, such as those encoding GST-1 and UDP glucuronosyltransferase show mild but significant increases. C3h-dioxin-inducible cytosolic aldehyde dehydrogenase-3, Cytochrome c oxidase Vb, and lactate dehydrogenase are also upregulated. Fourth, among growth-factor-related genes, those encoding the hepatocyte-growth factor-like protein shows significant upregulation, associated with a slight increase/decrease in expression level, with less significant p-values, for the following genes: fibroblast growth factor (FGF)-15, FGF-b, G protein-coupled receptor, growth factor-induced delayed-early-response protein, insulin-like growth factor 1 receptor precursor, insulin-induced growth response protein cl-6, tumor growth factor (TGF)-beta 1, TGF-beta 1 masking protein, and tumor necrosis factor alpha. Fifth, among the gene expression profiling of oncogenes, RhoB, which is possibly related to the genotoxic effect of benzene metabolites, shows a high expression level. Finally, hemopoiesis-related genes also show particular changes in their expression level, but the profiling of such genes led to the elucidation that benzene generally induces suppression of cell proliferation without an increase in cytokine gene expression levels.

TABLE 3.—*p53*-related genes whose expression level decreased or increased by benzene exposure, but unchanged in the wild-type mice.

WT: unchanged *p53*-KO: decreased	CalDAG-GEFI, Cbfa2, Dctn1, Frl, Grl-1, Ig/EBP, Klra3, Mek5, MEP, Mlp1, B-myb, Nog, PBX2, Prkm3, PTPalpha, Rad50, Rad51, Zfp94
WT: unchanged *p53*-KO: increased	24p3, 4E-BP2, Abcg2, ACRP, Activine, Ahd3, Alp, Anx3, AOE372, Apaf1, BAG-1, BAP, bcl-2, Calcyclin, Canexin, Caspase 9, Caspase 9S, CCR1, CD3 theta, CD71, CD143, Cox5b, Cox7a1, COX8H, Ctla-2a, Cu/Zn-SOD, Cyclin B1, DCIR, Dnmt2, Dpagt2, E4BP4, EPO, FACS, Fes, elk1, G6PD, G6PD-2, Galbp, Gapdh, Gcdh, Gdi2, Growth hormone, Gnb-1, Gng3lg, H-2T18, HES-1, IGF-1, IL1bc, IL-4, IL-9, JSR1, LDH-1, LDH-2, mLigI, Lipo 1, Lrf, Ly-3, Ly-40, Jam, JNK2, Kcc1, KSR1, M-CSF, Mac-1 alpha, Mch6, Mgl1, MHR23A, MmCEN3, Mrad17, MRP14, Mtx2, NFATp, NL, Nmo1, OERK, PAFR, Pde8, PERK, PGRP, Pla2g2c, PLGF, Pop2, Prkm9, Prtn3, RBP-L, Rga, S100A13, Siva, Smad 6, SPRR2J, Stat4, Stat 5B, TCF4, TOM1, Trypsin 2, Tst

See reference, Yoon et al. (2003).

It is of interest to determine gene expression in *p53*-KO mice with or without exposure by benzene inhalation (Yoon et al., 2003). In Table 3, the annotated genes were all downregulated (top) or upregulated (bottom) after benzene exposure, although their expressions were not altered in the wild-type mice, implying that the expressions of these genes are masked by the homeostasis governed by *p53* gene regulation. Thus, this study on *p53*-KO mice led to the elucidation of hidden gene alterations in wild-type mice, which we do not generally observe in toxicological examination.

REFERENCES

Boley, S. E., Wong, V. A., French, J. E., and Recio, L. (2002). *p53* heterozygosity alters the mRNA expression of *p53* target genes in the bone marrow in response to inhaled benzene. *Toxicol Sci* **66**, 209–15.

Cronkite, E. P., Bullis, J., Inoue, T., and Drew, R. T. (1984). Benzene inhalation produces leukemia in mice. *Toxicol Appl Pharmacol* **75**, 358–61.

Cronkite, E. P., Drew, R. T., Inoue, T., Hirabayashi, Y., and Bullis, E. (1989). Hematotoxicity and carcinogenicity of inhaled benzene. *Environ Health Perspect* **82**, 97–108.

Cronkite, E. P., Inoue, T., Carsten, A. L., Miller, M. E., Bullis, J. E., and Drew, R. T. (1982). Effects of benzene inhalation on murine pluripotent stem cells. *J Toxicol Environ Health* **9**, 411–21.

Farris, G. M., Robinson, S. N., Gaido, K. W., Wong, B. A., Wong, V. A., Hahn, W. P., and Shah, R. S. (1997). Benzene-induced hematotoxicity and bone marrow compensation in B6C3F1 mice. *Fundam Appl Toxicol* **36**, 119–29.

French, J. E., Lacks, G. D., Trempus, C., Dunnick, J. K., Foley, J., Mahler, J., Tice, R. R., and Tennant, R. W. (2001). Loss of heterozygosity frequency at the *Trp53* locus in *p53*-deficient (+/−) mouse tumors is carcinogen- and tissue-dependent. *Carcinogenesis* **22**, 99–106.

Hirabayashi, Y., Matsumura, T., Matsuda, M., Kuramoto, K., Motoyoshi, K., Yoshida, K., Sasaki, H., and Inoue, T. (1998). Cell kinetics of hemopoietic colony-forming units in spleen (CFU-S) in young and old mice. *Mech Ageing Dev* **101**, 221–31.

Hirabayashi, Y., Yoon, B. I., Kawasaki, Y., Li, G. X., Kanno, J., and Inoue, T. (2002). On the mechanistic differences of benzene-induced leukemogenesis between wild type and *p53* knockout mice. *Molecular Mechanisms for Radiation-Induced Cellular Response and Cancer Development* (K. Tanaka, T. Takabatake, K. Fujikawa, T. Matsumoto, and F. Sado, eds.), pp. 110–16. Aomori, Institute for Environmental Sciences, Japan.

Ho, T. Y., and Witz, G. (1997). Increased gene expression in human promyeloid leukemia cells exposed to trans, trans-muconaldehyde, a hematotoxic benzene metabolite. *Carcinogenesis* **18**, 739–44.

Irons, R. D., Heck, H., Moore, B. J., and Muirhead, K. A. (1979). Effects of short-term benzene administration on bone marrow cell cycle kinetics in the rat. *Toxicol Appl Pharmacol* **51**, 399–409.

Kawasaki, Y., Hirabayashi, Y., Yoon, B. I., Huo, Y., Kaneko, T., Kurokawa, Y., and Inoue, T. (2001). Benzene inhalation induced an early onset and a high incidence of leukemias in the *p53* deficient C57BL/6 mice. *Jpn J Cancer Res* **92**(Suppl), 71.

Lee, E. W., Garner, C. D., and Johnson, J. T. (1988). A proposed role played by benzene itself in the induction of acute cytopenia: inhibition of DNA synthesis. *Res Commun Chem Pathol Pharmacol* **60**, 27–46.

Le Noir and Claude (1897). Sur un cas de purpura atribué a l'intoxication par la benzine. *Bull Med Soc Hop Paris* **14**, 1251–60.

Li, G. X., Hirabayashi, Y., Yoon, B. I., Kawasaki, Y., Kurokawa, Y., Yodoi, J., Kanno, J., and Inoue, T. (2003). Benzene-induced leukemia is prevented by over-expression of Trx/ADF, along with increase in Trx/ADF-expression, increase in SOD-activity, and decrease in micronuclei. *Cancer Science* **94**(suppl), 265.

Mimura, J., Yamashita, K., Nakamura, K., Morita, M., Takagi, T. N., Nakao, K., Ema, M., Sogawa, K., Yasuda, M., Katsuki, M., and Fujii-Kuriyama, Y. (1997). Loss of teratogenic response to 2,3,7,8-tetrachlorodibenzo-*p*-dioxin (TCDD) in mice lacking the Ah (dioxin) receptor. *Genes Cells* **2**, 645–54.

Moeschlin, S., and Speck, B. (1967). Experimental studies on the mechanism of action of benzene on the bone marrow (radioautographic studies using 3H-thymidine). *Acta Haematol* **38**, 104–11.

Schattenberg, D. G., Stillman, W. S., Gruntmeir, J. J., Helm, K. M., Irons, R. D., and Ross, D. (1994). Peroxidase activity in murine and human hematopoietic progenitor cells: potential relevance to benzene-induced toxicity. *Mol Pharmacol* **46**, 346–51.

Snyder, C. A., Goldstein, B. D., Sellakumar, A. R., Bromberg, I., Laskin, S., and Albert, R. E. (1980). The inhalation toxicology of benzene: incidence of hematopoietic neoplasms and hematotoxicity in ARK/J and C57BL/6J mice. *Toxicol Appl Pharmacol* **54**, 323–31.

Tsukada, T., Tomooka, Y., Takai, S., Ueda, Y., Nishikawa, S., Yagi, T., Tokunaga, T., Takeda, N., Suda, Y., Abe, S., Matsuo, I., Ikawa, Y., and Aizawa, S. (1993). Enhanced proliferative potential in culture of cells from *p53*-deficient mice. *Oncogene* **8**, 3313–22.

Yoon, B. I., Hirabayashi, Y., Kawasaki, Y., Kodama, Y., Kaneko, T., Kim, D. Y., and Inoue, T. (2001). Mechanism of action of benzene toxicity: cell cycle suppression in hemopoietic progenitor cells (CFU-GM). *Exp Hematol* **29**, 278–85.

Yoon, B. I., Hirabayashi, Y., Kawasaki, Y., Kodama, Y., Kaneko, T., Kanno, J., Kim, D. Y., Fujii-Kuriyama, Y., and Inoue, T. (2002). Aryl hydrocarbon receptor mediates benzene-induced hematotoxicity. *Toxicol Sci* **70**, 150–6.

Yoon, B. I., Li, G. X., Kitada, K., Kawasaki, Y., Igarashi, K., Kodama, Y., Inoue, T., Kobayashi, K., Kanno, J., Kim, D. Y., and Hirabayashi, Y. (2003). Mechanisms of benzene-induced hematotoxicity and leukemogenicity: cDNA microarray analyses using mouse bone marrow tissue. *Environ Health Perspect* **111**, 1411–20.

Zhang, S., Cawley, G. F., Eyer, C. S., and Backes, W. L. (2002). Altered ethylbenzene-mediated hepatic CYP2E1 expression in growth hormone-deficient dwarf rats. *Toxicol Appl Pharmacol* **179**, 74–82.

Available online at www.sciencedirect.com
SCIENCE DIRECT®
Journal of Steroid Biochemistry & Molecular Biology 91 (2004) 121–129
The Journal of Steroid Biochemistry & Molecular Biology
www.elsevier.com/locate/jsbmb

Identification of estrogen-responsive genes in the GH3 cell line by cDNA microarray analysis

Nariaki Fujimoto [a,*], Katsuhide Igarashi [b], Junn Kanno [b], Hiroaki Honda [a], Tohru Inoue [b]

[a] *Department of Developmental Biology, Research Institute for Radiation Biology and Medicine (RIRBM), Hiroshima University, 1-2-3 Kasumi, Minami-ku, Hiroshima 734-8553, Japan*

[b] *Biological Safety Research Center, National Institute of Health Sciences, Kamiyoga 1-18-1, Setagaya-ku, Tokyo 158-8501, Japan*

Received 20 October 2003; accepted 27 February 2004

Abstract

To identify estrogen-responsive genes in somatolactotrophic cells of the pituitary gland, a rat pituitary cell line GH3 was subjected to cDNA microarray analysis. GH3 cells respond to estrogen by growth as well as prolactin synthesis. RNAs extracted from GH3 cells treated with 17β-estradiol (E2) at 10^{-9} M for 24 h were compared with the control samples. The effect of an antiestrogen ICI182780 was also examined. The array analysis indicated 26 genes to be up-regulated and only seven genes down-regulated by E2. Fourteen genes were further examined by real-time RT-PCR quantification and 10 were confirmed to be regulated by the hormone in a dose-dependent manner. Expression and regulation of these genes were then examined in the anterior pituitary glands of female F344 rats ovariectomized and/or treated with E2 and 8 out of 10 were again found to be up-regulated. Interestingly, two of the most estrogen-responsive genes in GH3 cells were strongly dependent on E2 in vivo. #1 was identified as calbindin-D9k mRNA, with 80- and 118-fold induction over the ovariectomized controls at 3 and 24 h, respectively, after E2 administration. #2 was found to be parvalbumin mRNA, with 30-fold increase at 24 h. Third was c-*myc* mRNA, with 4.5 times induction at 24 h. The levels were maintained after one month of chronic E2 treatment. Identification of these estrogen-responsive genes should contribute to understating of estrogen actions in the pituitary gland.

Keywords: Estrogen-responsive genes; cDNA microarray; Pituitary; GH3; Rats

1. Introduction

Estrogen regulates multiple functions in different cell types in the anterior pituitary gland [1–3]. In the somatolactotrophs (GH/prolactin cells), it is well documented that estrogen activates prolactin mRNA transcription through the estrogen-responsive element (ERE) located in the 5′-upstream regulatory region [4,5]. The storage and release of prolactin are also regulated by estrogen [6]. In addition to hormone production, estrogen promotes cell proliferation in somatolactotrophs, which is prominent in the rat case [7–9]. Although estrogen-responsive expression of a series of genes must be involved in these biological functions of the pituitary cells, only a few have so far been reported to be regulated by estrogen [2].

GH3 is a widely used rat pituitary somatolactotrophic cell line, originally isolated from the MtT/W5 pituitary tumor, whose growth and prolactin synthesis are stimulated by estrogen [10,11]. There is a variation in the estrogen-responsiveness of this cell line reported in the literature [5,12–15], but the cells obtained from the Health Science Research Resources Bank in Osaka, Japan, display high sensitivity with regard to induction of cell proliferation. In the present study, we performed a gene expression analysis of estrogen action in GH3 cells using the cDNA microarray technique and found many of the identified estrogen-responsive genes to also be similarly regulated in vivo in the anterior pituitary in F344 rats.

2. Materials and methods

2.1. Chemicals

17β-estradiol (E2) was purchased from Sigma Chemicals, St. Louis, MO, USA and ICI182780 was obtained from Tocris Cookson Ltd., Bristol, UK. Each was dissolved in

* Corresponding author. Tel.: +81 82 257 5820; fax: +81 82 256 7107.
E-mail address: nfjm@hiroshima-u.ac.jp (N. Fujimoto).

0960-0760/$ – see front matter © 2004 Elsevier Ltd. All rights reserved.
doi:10.1016/j.jsbmb.2004.02.006

ethanol to give stock solutions. Actinomycin D and cycloheximide were purchased from Wakojunyaku KK, Osaka, Japan.

2.2. Cell culture

The pituitary cell line GH3 was obtained from the Health Science Research Resources Bank (Osaka, Japan) and maintained in DME/F12 mixed medium (Sigma Chemical Co.) containing penicillin and streptomycin with 10% horse serum (HS, Gibco/Invitrogen Corp., Carlsbad, CA, USA) and 2.5% fetal bovine serum (FBS, Gibco/Invitrogen). Before estrogen treatment, cells were maintained for a week in phenol red-free medium (Sigma Chemicals) containing the same antibiotics along with dextran-charcoal-treated serum. For cell growth assays, GH3 cells were seeded in 24-well plates at 1×10^4 cells/well, and hormones were added the next day. Growth was measured after five days by means of a modified MTT assay with WST-1 (Dojindo Chemicals, Kumamoto, Japan). For microarray analysis, 3×10^6 GH3 cells were seeded in 90 mm dishes and treated with E2 at 10^{-9} M and/or ICI at 10^{-7} M and harvested after 24 h treatment. Cells were harvested after addition of Isogen (Wakojunyaku). For mRNA quantification, cells were treated with E2 at 10^{-12} to 10^{-9} M and/or ICI182780 at 10^{-7} M. After the indicated period of time, cells were harvested with cell lysis buffer supplied with an SV-total RNA isolation kit (Promega Co., Madison, WI, USA).

2.3. Animals

Animal experiments were conducted under the guidelines of the 'A Guide for the Care and Use of Laboratory Animals of Hiroshima University'. Female F344 rats were purchased at four weeks of age from Charles River Japan Co. (Kanagawa, Japan). They were maintained with free access to basal diet and tap water. All animals except the intact control underwent surgical ovariectomy upon receipt and implanted with pellets containing 10 mg of E2 subcutaneously as described previously [16]. Animals were sacrificed under ether anesthesia after 3, 8, 24 and 48 h in the short-term experiment. Treatment was extended between 7 and 30 days for the long-term experiment. The pituitary gland and the uterus of each rat were weighed and immediately frozen in liquid nitrogen and stored at −80 °C.

2.4. The GeneChip analysis

Total RNAs were extracted with Isogen, a premixed RNA isolation reagent, based on the acid guanidium thiocyanate–phenol–chloroform extraction method. The supplied protocol was followed.

First-strand cDNA was synthesized by incubating 5 μg of total RNAs with 200 U SuperScript II reverse transcriptase (Invitrogen, Carlsbad, CA), 100 pmol T7-(dT)24 primer [5′-GGCCAGTGAATTGTAATACGACTCACTATAGGGAGGCGG-(dT)24-3′], 1 × first-strand buffer (50 mM Tris–HCl pH 8.3, 75 mM KCl, 3 mM MgCl2, 10 mM DTT) and 0.5 mM dNTPs at 42 °C for 1 h. Second-strand synthesis was performed by incubating the first-strand cDNAs with 10 U *E. coli* ligase (Invitrogen), 40 U DNA polymerase I (Invitrogen), 2 U RNase H (Invitrogen), 1× reaction buffer (18.8 mM Tris–HCl pH 8.3, 90.6 mM KCl, 4.6 mM $MgCl_2$, 3.8 mM DTT, 0.15 mM NAD, 10 mM $(NH_4)_2SO_4$) and 0.2 mM dNTPs at 16 °C for 2 h. Ten units of T4 DNA polymerase (Invitrogen) were then added, and the reaction was allowed to continue for another 5 min at 16 °C. After phenol–chloroform extraction and ethanol precipitation, the double-stranded cDNA was resuspended in 12 μl DEPC-treated dH_2O. Labeling of the dsDNA was achieved by in vitro transcription using a BioArray HighYield RNA transcript labeling kit (Enzo Diagnostics, Farmingdale, NY). Briefly, the dsDNA was mixed with 1× HY reaction buffer, 1× biotin labeled ribonucleotides (NTPs with Bio-UTP and Bio-CTP), 1× DTT, 1× RNase inhibitor mix and 1× T7 RNA polymerase. The mixture was incubated at 37 °C for 4 h. The labeled cRNA was then purified using a RNeasy mini kit (Qiagen, Valencia, CA) according to the manufacturer's instructions. The purified cRNA was fragmented in 1 × fragmentation buffer (40 mM acetate, 100 mM KOAc, 30 mM MgOAc) at 94 °C for 35 min. For hybridization with the GeneChip Rat Genome U34A (Affymetrix), 15 μg fragmented cRNA probe was incubated with 50 pM control oligonucleotide B2, 1× eukaryotic hybridization control (1.5 pM BioB, 5 pM BioC, 25 pM BioD and 100 pM Cre), 0.1 mg/ml herring sperm DNA, 0.5 mg/ml acetylated BSA and 1× manufacturer-recommended hybridization buffer in a 45 °C rotisserie oven for 16 h. Washing and staining were performed with a GeneChip Fluidic Station (Affymetrix) using the appropriate antibody amplification washing and staining protocol. The phycoerythrin-stained arrays were scanned as digital image files and scanned data were analyzed with GeneChip software (Affymetrix) [17].

2.5. Quantification of mRNAs by real-time RT-PCR

RNA preparation was carried out with an SV-total RNA isolation kit. One microgram of total RNA was reverse-transcribed with 200 U of MMLV-RT (Invitrogen) and 2.5 pmol of oligo-dT primer (Invitrogen) in 25 μl buffer containing 1 mM dNTP, 100 mM Tris–HCl (pH 8.3), 150 mM KCl, 6 mM $MgCl_2$, 60 mM dithiothreitol and 5 U/μl RNasin with incubation at 37 °C for 60 min.

The real-time PCR method with a QuantiTect Sybr Green PCR kit (Qiagen) and an ABI Prism 7700 (The Perkin–Elmer Co) was employed for quantitative measurement for following the supplied protocol [18]. Specific primer sets with a T_m of about 59 °C were designed for each mRNA selected from the microarray analysis (Table 1). The PCR conditions were a 15 min of initial activation step followed by 45 cycles of 15 s at 94 °C, 30 s at 50 °C and 60 s at

Table 1
Nucleotide sequences of primers for quantitative real-time PCR

Gene	GenBank accession#	Forward	Reverse
#1	K00994	AACCAGCTGTCCAAGGAGGA	CTTCTCCATCATCGTTCTTATCCA
#2	AI175539	TTTCTTCAGGCCCACCATCT	TTGCAGGATGTCGATGACAGA
#3	AI014135	GAACCAATTCTCCTAGCACAAGTG	CACGCCTGTGTTGGGCTAA
#4	AI178971	GGTGTGAAATCCCCAGGGT	CCCTGTCCACTCTGAGCGAC
#5	S81478	GATCAACGTCTCGGCCAATT	GCACAAACACCCTTCCTCCA
#6	D26393	GATTTCTAGGCGGTTCCGGA	ACTCGGAGCACACGGAAGTT
#7	AI230712	TGGCAGAAAAATCAATCCAGC	AAAGCCAGCCCCAAATCAC
#8	AF081366	CATCTGGACAACTGTGCTGGA	GGCACCACACATGAAGGAATT
#9	Y00396	CCGAGCTACTTGGAGGAGACA	AGGCCAGCTTCTCGGAGAC
#10	U02553	GATCAACGTCTCGGCCAATT	GCACAAACACCCTTCCTCCA
#14	U24175	CAGTGGATCGAGAGCCAGC	TGCCCCAGCTTGATCTTCAG
#15	D13623	ACCAAGACCGGTAGCAAGGG	GAAATCCGACGGAAGAGTGC
#21	AA892522	CCTTCGACTCAGCCACAAAAA	ACAGGGTCTTACCCTGCCTTC
#22	L16922	AGCCAGAGCCCACAATATGG	GCAATCATTTCTTCCGGCAC
G3PDH	AB017801	TGAAGGTCGGTGTGAACGGATTTG	TGATGGCATGGACTGTGGTCATGA

72 °C. Prior to the quantitative analysis, PCR products were prepared separately and purified by gel electrophoresis. The fragments extracted from the gel were used as standards for quantification. The DNA sequences were confirmed with a capillary DNA sequencer, ABI 310 (The Perkin–Elmer Co.). All mRNA contents were normalized with reference to G3PDH mRNA.

2.6. Statistical analysis

Multiple comparison was made by ANOVA followed by Scheffe's test. Otherwise, Student's *t*-test was applied.

3. Results

3.1. Estrogen-dependent cell proliferation of GH3

The relative cell numbers were measured at day 5 of treatment with E2 at concentrations from 10^{-13} to 10^{-9} M (Fig. 1). Significant stimulation of cell proliferation was observed at 10^{-12} M and the response appeared to reach a maximum at 10^{-11} M. The sizes of individual cells treated with E2 appeared to be larger than without hormone.

3.2. Estrogen-responsive genes identified by cDNA microarray

Differentially expressed genes based on the ratio of the measured hybridization intensities on GeneChip Rat Genome U34A between control and E2-treated cells are listed in Table 1. A minimal change of two-fold was applied to select up- and down-regulated genes. Two independent experiments were carried out and the genes showing reliable hybridization for both experiments were counted. The genes are listed according to average values of E2 induction. The results of ICI182780 treatment alone or with E2 are also given in Table 2. The genes regulated by E2 but not showing inhibition by ICI182780, which only accounted for four in total, are not included in the table. Interestingly, only 26 genes were categorized as up-regulated and seven as the down-regulated, out of approximately 8000 genes on the chip.

3.3. Confirmation of mRNA changes

From Table 2, the top ten genes and four others (#14, #15, #21 and #22) were selected and subjected to quantification of mRNA levels to confirm the results of cDNA microarray analysis. cDNAs from GH3 cells treated with E2 at 10^{-12} to 10^{-9} M and/or ICI at 10^{-7} M are examined and

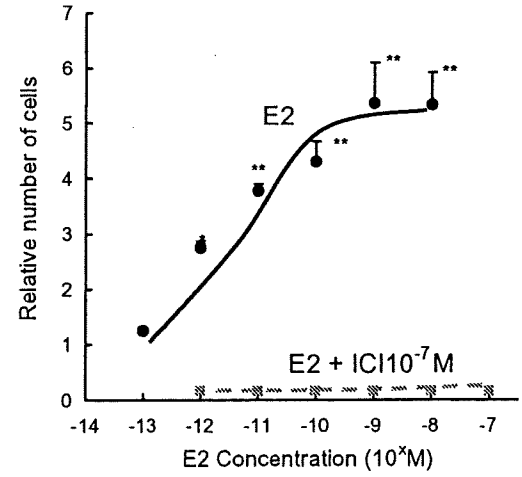

Fig. 1. Effects of 17β-estradiol (E2) and ICI182780 (ICI) on GH3 cell proliferation. Cells were seeded in 24-well plates at 1×10^4 cells per well. After five days treatment with E2 at 10^{-13} to 10^{-9} M alone or with ICI at 10^{-7} M, cell proliferation was measured by a modified MTT assay. Each point represents a mean ± S.E.M. ($n = 4$). *,** Indicates significant differences from the control value at 0.05 and 0.01, respectively.

Table 2
Genes up- and down-regulated by estrogen two or more fold in the microarray study

Genbank accession#		Gene name/blast match	Fold change in expression			
			E2(Exp1)	E2(Exp2)	E2+ICI	ICI
Genes up-regulated						
#1	K00994	Calbindin-D9k*	8.12	6.20	0.70	0.33
#2	AI175539	Parvalbumin*	7.58	4.54	0.81	0.28
#3	AI014135	Ribosomal RNA*	6.23	4.93	1.17	0.94
#4	M17083	Alpha globin*	5.23	4.99	0.39	0.59
#5	S81478	3CH134/CL1 ATPase	4.77	4.12	0.97	1.11
#6	D26393	Type II hexokinase	2.75	3.15	0.14	0.49
#7	AI230712	PACE4*	2.98	2.73	0.44	0.15
#8	AF081366	K + channel ROMK2.1 isoform	3.21	2.44	0.88	0.20
#9	Y00396	c-*myc* protein	2.99	2.59	0.76	0.35
#10	U02553	Protein tyrosine phosphatase	3.32	2.23	0.67	0.44
#11	AF036548	RGC-32	3.47	2.05	1.12	0.37
#12	U53505	Type II iodothyronine deiodinase	2.26	2.87	0.77	0.34
#13	Y09507	Hypoxia-inducible factor 1	2.60	2.38	1.13	0.69
#14	U24175	Regulator of transcription 5a1	2.77	2.01	0.61	0.46
#15	D13623	p34 protein	2.43	2.32	1.05	1.02
#16	M58040	Transferrin receptor	2.37	2.38	0.73	0.30
#17	AA819776	EST (similar to HSP86)	1.93	2.76	1.82	1.97
#18	AA875126	EST (unknown)	2.33	2.27	0.58	0.70
#19	M14656	Osteopontin	1.89	2.69	1.37	1.22
#20	X67788	Ezrin, p81	2.28	2.23	0.47	0.50
#21	AA892522	EST (unknown)	2.19	2.23	0.60	0.82
#22	L16922	Progesterone receptor	2.30	2.04	0.89	0.67
#23	U57097	APEG-1 protein	2.36	1.97	1.43	1.51
#24	M24852	Neuron-specific protein	1.87	2.45	1.73	1.57
#25	AA817846	EST (similar to D-β-hydroxy butyrate dehydrogenase)	1.86	2.37	0.97	0.96
#26	AI169417	Phosphoglycerate mutase type B subunit mRNA*	1.98	2.23	0.97	0.92
Genes down-regulated						
	U67080	Zinc finger protein r-MyT3	0.49	0.47	1.38	1.06
	AA799964	EST (unknown)	0.49	0.41	0.51	0.71
	AI639263	EST (unknown)	0.46	0.41	0.68	0.32
	M27925	Synapsin 2a	0.47	0.35	1.31	1.31
	E03229	JP 1991272688-A/2	0.47	0.30	1.31	0.95
	AI237654	Vdup1*	0.40	0.35	0.81	0.84
	AA893280	EST (similar to adipose differenti-ation-related protein)	0.47	0.21	0.91	0.98

Gene are listed in order of average E2 fold change in Experiments 1 and 2. **Four E2 up-regulated genes were not inhibited by ICI, which are not included in this table (The GenBank accession numbers of these are AI138070, AA866485, D84480 and X74293).
* Indicates genes originally listed as ESTs but found to have perfect match by BLAST.

the results were summarized in Fig. 2. Although the fold increases of E2 induced gene expression were slightly lower than in the microarray analysis, up-regulation and inhibition by ICI182780 were confirmed except with three genes, #3, #6 and #15, which showed no responses. Time dependence of gene expression induced by E2 was also examined and the results are summarized in Fig. 3. As expected, some of the genes were expressed early after E2 administration and others increased gradually. Since the microarray analysis was carried out at only one time point, 24 h after E2 treatment, early responding and quickly muting genes would not be expected to be identified.

To determine E2 in inducing the transcription of genes #1 and #2, GH3 cells were treated with E2 in the presence of 0.5 μg/ml of actinomycin D (a transcription inhibitor) and 10 μg/ml cycloheximide (a translation inhibitor) for 3 and 24 h (Table 3). Increase in mRNA levels by E2 was blocked

Table 3
Effects of cycloheximide and actinomycin D on E2-induced mRNA change of calbindin D9k and parvalbumin in GH3 cells

	3 h	24 h
Gene#1: calbindin D9k		
Control	5.45 ± 0.70**	4.02 ± 0.33**
CHX	4.03 ± 0.11**	3.74 ± 0.27**
ActD	1.01 ± 0.21	1.13 ± 0.23
Gene#2: parvalbumin		
Control	1.81 ± 0.41	4.52 ± 0.94*
CHX	2.51 ± 0.19**	8.34 ± 0.37**
ActD	0.93 ± 0.09	1.58 ± 0.31

Cell were treated with E2 at 10^{-9} M for 3 and 24 h with or without cycloheximide (CHX) at 10 μg/ml or actinomycin D (ActD) at 0.5 μg/ml. The inductions by E2 were calculated for each treatment (mean ± S.E.M., $n = 4$).
* Indicates significant induction at 0.05 and 0.01, respectively.
** Indicates significant induction at 0.05 and 0.01, respectively.

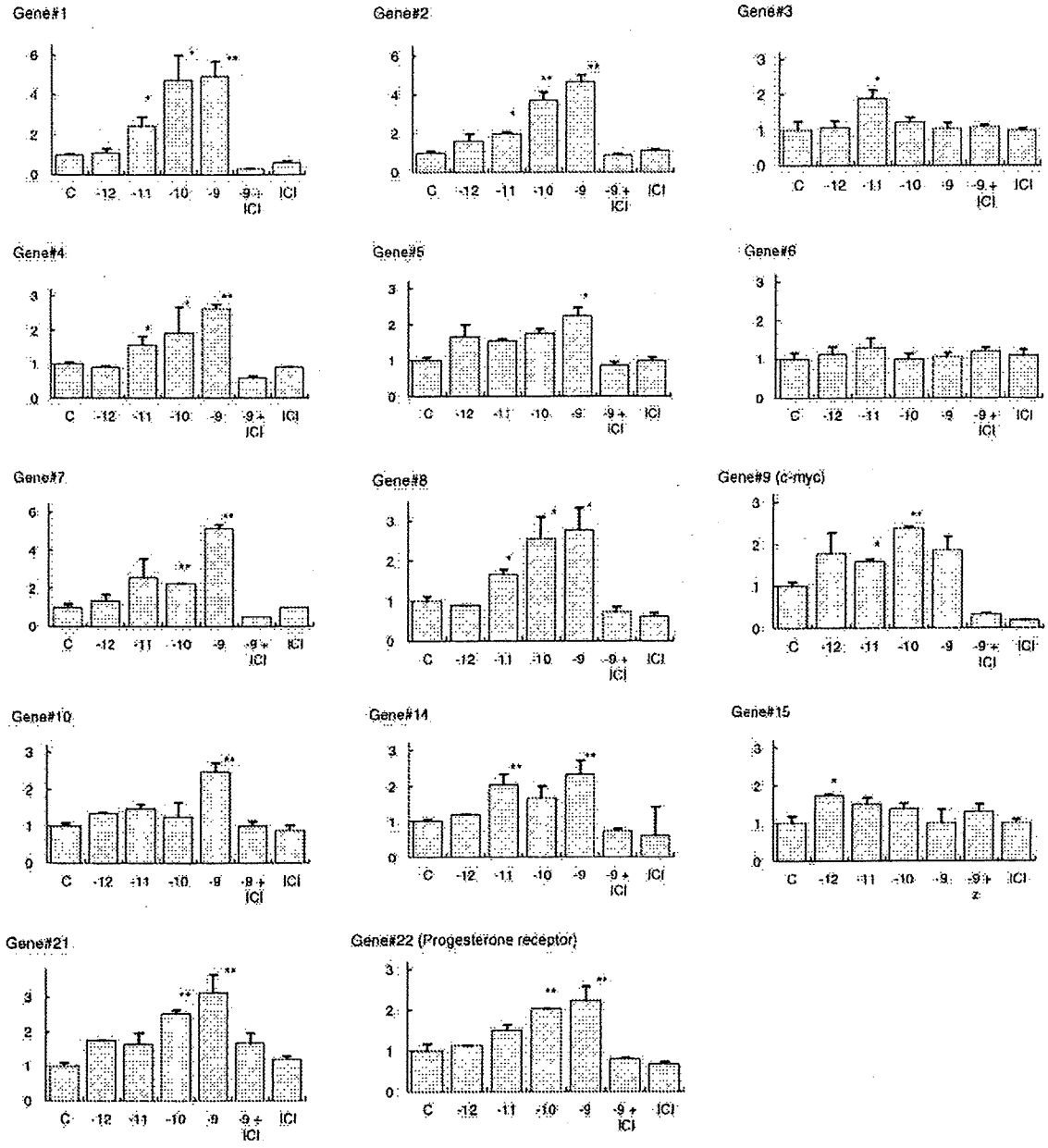

Fig. 2. Dose-dependent changes in gene expression levels measured by quantitative real-time RT-PCR. Cells were treated with different concentrations of E2 at 10^{-12} to 10^{-9} M and/or a single dose of ICI 182780 (ICI) at 10^{-7} M for 24 h. All mRNA contents were normalized with reference to G3PDH mRNA. The fold changes were calculated based on the gene expression in the cells treated with vehicle. Each point is an average of two independent experiments.

by actinomycin D but not by cycloheximide, which indicates that E2 regulates these genes at the transcriptional level.

3.4. Expression of genes in the pituitary gland

Expression of estrogen regulated genes in GH3 cells was further investigated in the anterior pituitary gland. First, mRNA expression of eleven-responsive genes was examined in short-term (24 h) and long-term (30 days) E2-treated ovariectomized F344 rats. Findings for estrogen-dependent increase for each gene are summarized in Table 4 as fold change of mRNA in E2-treated animals over that in the ovariectomized controls. All the genes except #4 were up-regulated in pituitary tissue by the short-term and long-term treatment of E2. Estrogen dependence of expression of gene #1 (calbindin-D9k) and gene #2 (parvalbumin) was extremely strong, over 100-fold induction being noted. For these and gene #9 (c-*myc*), more detailed time-dependent analysis was carried out. In Fig. 4, each mRNA level was calculated based on the level in ovariectomized rats at day

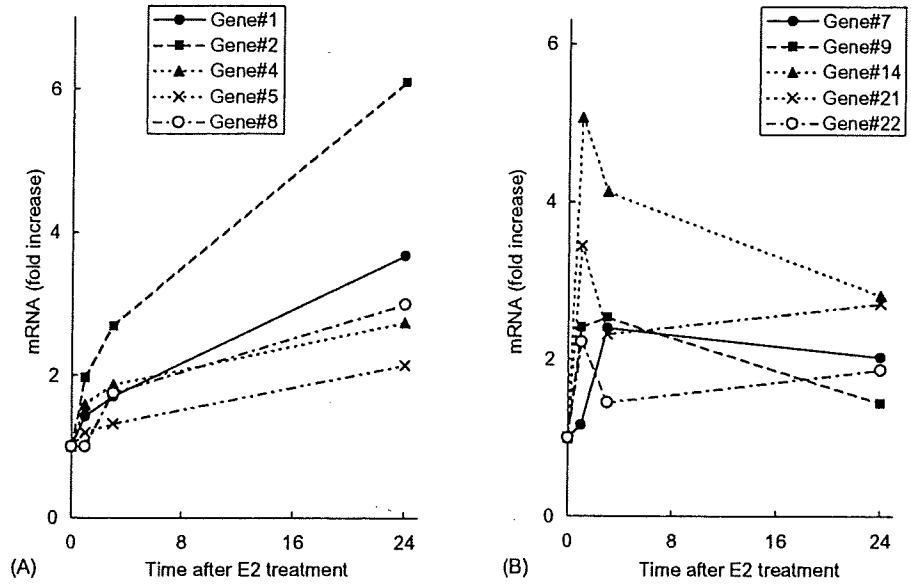

Fig. 3. Time-dependent change in gene expression levels measured by quantitative real-time RT-PCR. All mRNA contents were normalized with reference to G3PDH mRNA. Cells were treated with E2 at 10^{-9} M for 0, 1, 3 and 24 h. Each point represents a mean ± S.E.M. ($n = 4$). *,** Indicates significant differences from the control values at 0.05 and 0.01, respectively.

Table 4
Estrogen-responsive genes identified by the microarray study in the pituitary tissues in ovariectomized F344 rats

Gene	GenBank accession#	Fold change in expression	
		24 h	1 month
#1	K00994	118	95.0
#2	AI175539	28.9	70.0
#4	M17083	1.1	0.6
#5	S81478	2.3	2.0
#7	AI230712	2.9	4.7
#8	AF081366	9.9	2.0
#9	Y00396	4.5	17.7
#10	U02553	3.1	1.6
#14	U24175	2.4	4.0
#21	AA892522	2.0	5.1
#22	L16922	4.2	9.4

Ovariectomized F344 rats were treated subcutaneously with pellets containing E2 for 1 and 30 days. The gene expression was measured by quantitative real-time RT-PCR in pituitary tissue and the fold changes were calculated based on the mRNA level in ovariectomized controls at time 0 ($n = 5$).

0. All the three mRNAs, for calbindin-D9k, parvalbumin and c-*myc*, were induced significantly within 3 h of subcutaneous E2 administration, although the increase was most prominent for calbindin-D9k, with a 72-fold elevation. Higher levels were still maintained after a month of chronic E2 treatment.

4. Discussion

The GH3 cell line has been widely used to investigate the functions of somatolactotrophic cells, since regulation of its GH and prolactin production appears to be physiologically relevant with dependence on thyroid hormones, estrogen and glucocorticoid [11,12,19]. In the present study, we applied microarray analysis and identified a number of estrogen-responsive genes.

In terms of GH3 estrogen-responsiveness, there are two distinct parameters, prolactin synthesis and cell proliferation. However, reported sensitivity to estrogen has varied in the literature [4,13–15,20]. The inter-laboratory variation may be due partly to differences in strain, since GH3 has a rather old origin and has been widely used. Technical problems with charcoal treatment of serum for removing estrogenic substances may have had an impact in some cases [21]. The estrogenic activity of phenol red or related contaminants in common culture media was not recognized until Katzenellenbogen's group provided a convincing evidence [22]. Prior to the present microarray analysis, GH3 cells were examined in our culture conditions and found to be very sensitive to estrogen, exhibiting induction of cell proliferation in response to E2 at a concentration as low as 10^{-12} M. The high sensitivity on cell proliferation appears typical for pituitary cell lines, like the MtT/E-2 cell line we have established and another lactotrophic cell line, PR1 [4,23]. ERα is the major type of ER expressed in GH3 cells with a ratio to ERβ of 380:1 according to quantitative PCR (data not shown).

Recently, estrogen-responsive genes have been investigated by cDNA microarray in human breast cancers and the normal uterus [24,25]. However, the pituitary gland has not been explored for estrogen-responsive genes by this approach, to our knowledge. In the present microarray analysis, a relatively small number of genes were found to be

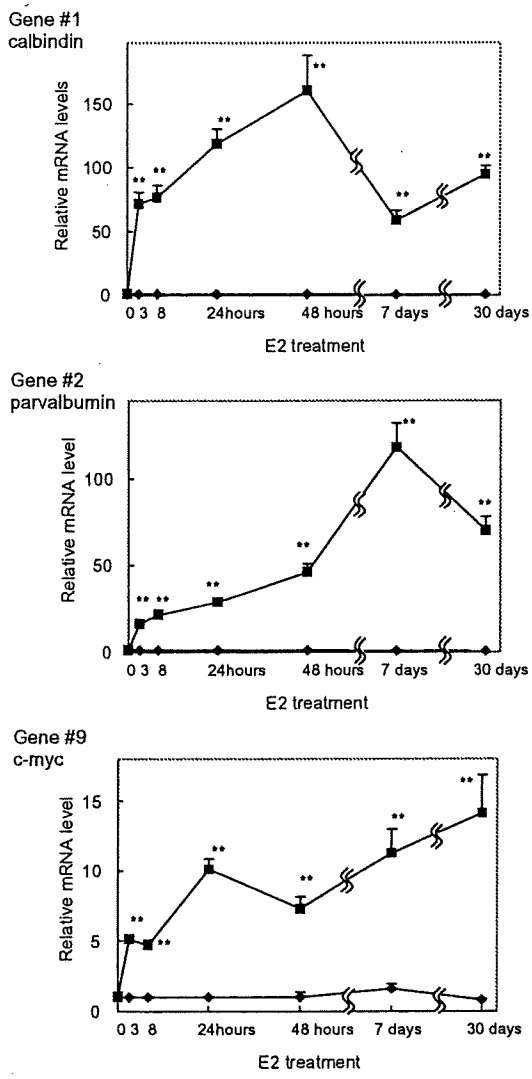

Fig. 4. Time-dependent analysis of three estrogen-responsive genes in the pituitary in vivo. Ovariectomized F344 rats were treated subcutaneously with pellets containing E2 for 3, 8, 24, and 48 h and 7 and 30 days. Gene expression was measured by quantitative real-time RT-PCR in pituitary tissue and fold changes were calculated based on the mRNA level in the ovariectomized controls at time zero. All mRNA contents were normalized with reference to G3PDH mRNA. Each point and bar represent mean ± S.E.M. ($n = 5$), *,** Indicates significant differences from the control values at 0.05 and 0.01, respectively.

regulated by estrogen with confirmation in most cases by quantitative real-time PCR. Suppression by ICI of E2-induced gene expression was also confirmed. The degrees of change were similar with real-time PCR analysis and GeneChip data and although we selected up-regulated genes after 24 h of estrogen exposure, some genes proved to be rapidly regulated (Fig. 3(B)) including these for the progesterone receptor and c-*myc*. Estrogen-responsive induction of progesterone receptor is well documented for the primary target, the uterus, as well as in the anterior pituitary gland [26,27]. Estrogen activation of c-*myc* also has been reported in the anterior pituitary gland and breast cancer cells [28,29]. A total of seven genes could be listed as down-regulated but they were not analyzed further, since all of them displayed relatively small degrees of change to 0.34–0.48 of the control values. Other known estrogen-responsive genes in the pituitary gland, such as prolactin and TGFα were not on the array used in the present study.

Interestingly, the in vivo expression of two genes, calbindin-D9k and parvalbumin, was found to be highly induced by E2 both in the short and longer term, which may suggest that hypothalamus or other indirect endocrine pathways would be involved in regulating genes in addition to the direct transcriptional activation. Calbindin-D9k is a vitamin D-dependent intestinal calcium-binding protein that is detectable in the duodenum, uterus and placenta [30–32]. Another vitamin D-dependent calcium-binding protein, calbindin-D28k, expressed in kidney and brain has no homology with calbindin-D9k either at the nucleotide or at the transcript levels [33]. The calbindin-D9k gene has been reported to contain a 15-base-pair imperfect palindrome with high homology to the estrogen- and glucocorticoid-responsive elements (ERE and GRE) [34]. Although there is no evidence that this protein is regulated by estrogen in the intestine through this motif, it is possible that the imperfect ERE is functional for the hormone-dependent transcription in the pituitary gland. Parvalbumin is another calcium-binding protein that belongs to the EF-hand calcium-binding protein like calbindin-D9k [35]. It is abundant in fast contracting/relaxing muscle fibers, where it plays a role as a calcium buffer and is also found in neurons as well as in endocrine glands including pituitary, thyroid, adrenals, testes and ovaries [36]. It has been postulated that parvalbumin can prevent cell death due to calcium overload in neurons. Although its expression is developmentally regulated in muscle, brain and other tissues, no evidence indicating hormonal regulation has been reported [37,38]. The 5′ flanking region of the gene seems to function as the promoter but it does not contain any motifs for estrogen-dependent transcription [39,40].

Since RNA was extracted from whole anterior pituitary tissue in the present study, it is not clear which types of cell actually contributed to the increase in mRNA levels. Chronic treatment of rats with E2 is known to result in the development of lactotrophic tumors [5]. The F344 strain is the most sensitive to E2 and somatolactotrophs of the pituitary become hyperplastic after exposure for a week and steadily proliferate thereafter. In the present study, major response of GH3 cells was cell proliferation so that some of the identified genes might be expected to be mitosis-related and involved in estrogen-induced pituitary hyperplasia/tumorigenesis. Although up-regulation of the calbindin-D9k and parvalbumin gene are evident on long-term treatment of E2, there was no obvious correlation with the time period for pituitary hyperplasia in contrast to the c-*myc* expression which steadily increase.

In conclusion, the present microarray analysis allowed identification of a number of estrogen-responsive genes in GH3 cells whose regulation appears biologically relevant in the pituitary gland in vivo. The actual significance of two calcium-binding proteins discovered to be prominently induced by E2 remains to be explored in the future.

Acknowledgements

We thank Mr. Y. Mizuno for his expert technical assistance and Dr. M.A. Moore for reading the manuscript and suggesting English clarification. This work was supported, in part, by Grant-in-Aid (H13-Seikatsu) from the Ministry of Health, Labor and Welfare, Japan and a Grant-in-Aid (#14042241) from the Ministry of Education, Culture, Sports, Science and Technology, Japan.

References

[1] W.L. Miller, M.M. Knight, J. Gorski, Estrogen action in vitro: regulation of thyroid stimulating and other pituitary hormones in cell cultures, Endocrinology 101 (1977) 1455–1460.
[2] K.M. Scully, A.S. Gleiberman, J. Lindzey, D.B. Lubahn, K.S. Korach, M.G. Rosenfeld, Role of estrogen receptor-alpha in the anterior pituitary gland, Mol. Endocrinol. 11 (1997) 674–681.
[3] D.L. Allen, N.A. Mitchner, T.E. Uveges, K.P. Nephew, S. Khan, J.N. Ben, Cell-specific induction of c-*fos* expression in the pituitary gland by estrogen, Endocrinology 138 (1997) 2128–2135.
[4] T.Y. Chun, D. Gregg, D.K. Sarkar, J. Gorski, Differential regulation by estrogens of growth and prolactin synthesis in pituitary cells suggests that only a small pool of estrogen receptors is required for growth, Proc. Natl. Acad. Sci. USA 95 (1998) 2325–2330.
[5] M.E. Lieberman, R.A. Maurer, P. Claude, J. Wiklund, N. Wertz, J. Gorski, Regulation of pituitary growth and prolactin gene expression by estrogen, Adv. Exp. Med. Biol. 138 (1981) 151–163.
[6] C.L. Bethea, Stimulatory effect of estrogen on prolactin secretion from primate pituitary cells cultured on extracellular matrix and in serum-free medium, Endocrinology 115 (1984) 443–451.
[7] T.J. Spady, K.L. Pennington, R.D. McComb, J.D. Shull, Genetic bases of estrogen-induced pituitary growth in an intercross between the ACI and Copenhagen rat strains: dominant mendelian inheritance of the ACI phenotype, Endocrinology 140 (1999) 2828–2835.
[8] S. Holtzman, J.P. Stone, C.J. Shellabarger, Influence of diethylstilbestrol treatment on prolactin cells of female ACI and Sprague-Dawley rats, Cancer Res. 39 (1979) 779–784.
[9] R.V. Lloyd, K. Coleman, K. Fields, V. Nath, Analysis of prolactin and growth hormone production in hyperplastic and neoplastic rat pituitary tissues by the hemolytic plaque assay, Cancer Res. 47 (1987) 1087–1092.
[10] J. Tashjian-AH, Y. Yasumura, L. Levine, G.H. Sato, M.L. Parker, Establishment of clonal strains of rat pituitary tumor cells that secrete growth hormone, Endocrinology 82 (1968) 342–352.
[11] J.M. Sorrentino, W.L. Kirkland, D.A. Sirbasku, Control of cell growth. II. Requirement of thyroid hormones for the in vivo estrogen-dependent growth of rat pituitary tumor cells, J. Natl. Cancer Inst. 56 (1976) 1155–1158.
[12] E. Haug, K.M. Gautvik, Effects of sex steroids on prolactin secreting rat pituitary cells in culture, Endocrinology 99 (1976) 1482–1489.
[13] D.R. Kiino, P.S. Dannies, Insulin and 17 beta-estradiol increase the intracellular prolactin content of GH4C1 cells, Endocrinology 109 (1981) 1264–1269.
[14] P.R. Rhode, J. Gorski, Growth and cell cycle regulation of mRNA levels in GH3 cells, Mol. Cell Endocrinol. 82 (1991) 11–22.
[15] J.G. Scammell, T.G. Burrage, P.S. Dannies, Hormonal induction of secretory granules in a pituitary tumor cell line, Endocrinology 119 (1986) 1543–1548.
[16] N. Fujimoto, H. Watanabe, A. Ito, K. Inoue, Estrogen receptor levels and tumor growth in a series of pituitary clonal cell lines in rats, Jpn. J. Cancer Res. 82 (1991) 1436–1441.
[17] D.J. Lockhart, H. Dong, M.C. Byrne, M.T. Follettie, M.V. Gallo, M.S. Chee, M. Mittmann, C. Wang, M. Kobayashi, H. Horton, E.L. Brown, Expression monitoring by hybridization to high-density oligonucleotide arrays, Nat. Biotechnol. 14 (1996) 1675–1680.
[18] T.H. Woo, B.K. Patel, M. Cinco, L.D. Smythe, M.L. Symonds, M.A. Norris, M.F. Dohnt, Real-time homogeneous assay of rapid cycle polymerase chain reaction product for identification of *Leptonema illini*, Anal. Biochem. 259 (1998) 112–117.
[19] E. Haug, O. Naess, K.M. Gautvik, Receptors for 17β-estradiol in prolactin-secreting rat pituitary cells, Mol. Cell Endocrinol. 12 (1978) 81–95.
[20] J.F. Amara, I.C. Van, P.S. Dannies, Regulation of prolactin production and cell growth by estradiol: difference in sensitivity to estradiol occurs at level of messenger ribonucleic acid accumulation, Endocrinology 120 (1987) 264–271.
[21] T.L. Riss, D.A. Sirbasku, Rat pituitary tumor cells in serum-free culture. II. Serum factor and thyroid hormone requirements for estrogen-responsive growth, In Vitro Cell Dev. Biol. 25 (1989) 136–142.
[22] Y. Berthois, J.A. Katzenellenbogen, B.S. Katzenellenbogen, Phenol red in tissue culture media is a weak estrogen: implications concerning the study of estrogen-responsive cells in culture, Proc. Natl. Acad. Sci. USA 83 (1986) 2496–2500.
[23] N. Fujimoto, S. Maruyama, A. Ito, Establishment of an estrogen-responsive rat pituitary cell sub-line MtT/E-2, Endocr. J. 46 (1999) 389–396.
[24] H. Watanabe, A. Suzuki, M. Kobayashi, E. Takahashi, M. Itamoto, D.B. Lubahn, H. Handa, T. Iguchi, Analysis of temporal changes in the expression of estrogen-regulated genes in the uterus, J. Mol. Endocrinol. 30 (2003) 347–358.
[25] A. Inoue, N. Yoshida, Y. Omoto, S. Oguchi, T. Yamori, R. Kiyama, S. Hayashi, Development of cDNA microarray for expression profiling of estrogen-responsive genes, J. Mol. Endocrinol. 29 (2002) 175–192.
[26] L.A. Denner, W.T. Schrader, B.W. O'Malley, N.L. Weigel, Hormonal regulation and identification of chicken progesterone receptor phosphorylation sites, J. Biol. Chem. 265 (1990) 16548–16555.
[27] E. Vegeto, M.M. Shahbaz, D.X. Wen, M.E. Goldman, B.W. O'Malley, D.P. McDonnell, Human progesterone receptor A form is a cell- and promoter-specific repressor of human progesterone receptor B function [see comments], Mol. Endocrinol. 7 (1993) 1244–1255.
[28] I. Szijan, D.L. Parma, N.I. Engel, Expression of c-*myc* and c-*fos* protooncogenes in the anterior pituitary gland of the rat. Effect of estrogen, Horm. Metab. Res. 24 (1992) 154–157.
[29] D. Dubik, R.P. Shiu, Mechanism of estrogen activation of c-*myc* oncogene expression, Oncogene 7 (1992) 1587–1594.
[30] A.C. Delorme, J.L. Danan, M.G. Acker, M.A. Ripoche, H. Mathieu, In rat uterus 17β-estradiol stimulates a calcium-binding protein similar to the duodenal vitamin D-dependent calcium-binding protein, Endocrinology 113 (1983) 1340–1347.
[31] M.E. Bruns, A. Fausto, L.V. Avioli, Placental calcium binding protein in rats. Apparent identity with vitamin D-dependent calcium binding protein from rat intestine, J. Biol. Chem. 253 (1978) 3186–3190.
[32] M. Davie, Calcium-ion-binding activity in human small-intestinal mucosal cytosol. Purification of two proteins and interrelationship of calcium-binding fractions, Biochem. J. 197 (1981) 55–65.